



The University of
Nottingham

UNITED KINGDOM · CHINA · MALAYSIA

Schwehm, Carolin and Kellam, Barrie and Garces, Aimie and Hill, Stephen J. and Kindon, Nicholas and Bradshaw, Tracey D. and Li, Jin and Macdonald, Simon J.F. and Rowedder, James E. and Stoddart, Leigh A. and Stocks, Michael (2017) Design and elaboration of a tractable tricyclic scaffold to synthesize druglike inhibitors of dipeptidyl peptidase-4 (DPP-4), antagonists of the C–C Chemokine Receptor Type 5 (CCR5), and highly potent and selective phosphoinositol-3 Kinase δ (PI3K δ) inhibitors. *Journal of Medicinal Chemistry*, 60 (4). pp. 1534-1554. ISSN 1520-4804

Access from the University of Nottingham repository:

<http://eprints.nottingham.ac.uk/44065/1/acs.jmedchem.6b01801.pdf>

Copyright and reuse:

The Nottingham ePrints service makes this work by researchers of the University of Nottingham available open access under the following conditions.

This article is made available under the University of Nottingham End User licence and may be reused according to the conditions of the licence. For more details see:

http://eprints.nottingham.ac.uk/end_user_agreement.pdf

A note on versions:

The version presented here may differ from the published version or from the version of record. If you wish to cite this item you are advised to consult the publisher's version. Please see the repository url above for details on accessing the published version and note that access may require a subscription.

For more information, please contact eprints@nottingham.ac.uk

Design and Elaboration of a Tractable Tricyclic Scaffold To Synthesize Druglike Inhibitors of Dipeptidyl Peptidase-4 (DPP-4), Antagonists of the C–C Chemokine Receptor Type 5 (CCR5), and Highly Potent and Selective Phosphoinositol-3 Kinase δ (PI3K δ) Inhibitors

Carolin Schwehm,[†] Barrie Kellam,[†] Aimie E. Garces,[†] Stephen J. Hill,[‡] Nicholas D. Kindon,[†] Tracey D. Bradshaw,[†] Jin Li,[§] Simon J. F. Macdonald,^{||} James E. Rowedder,^{||} Leigh A. Stoddart,[‡] and Michael J. Stocks^{*,†,§}

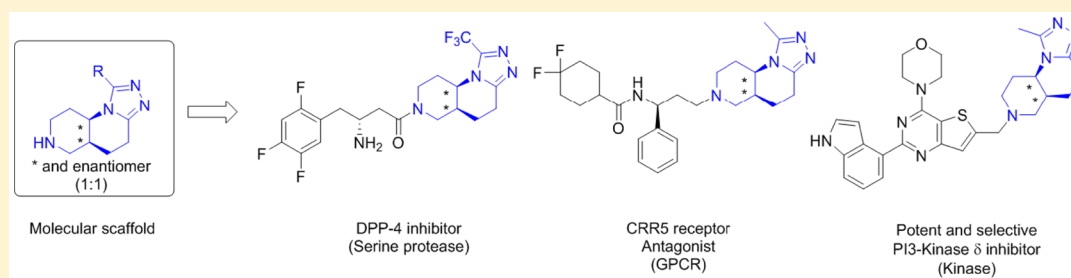
[†]School of Pharmacy, Centre for Biomolecular Sciences, University Park Nottingham, Nottingham, NG7 2RD, U.K.

[‡]Institute of Cell Signalling, Medical School, University of Nottingham, Nottingham, NG7 2UH, U.K.

[§]Hitgen Ltd., F7-10, Building B3, Tianfu Life Science Park, 88 South Kayuan Road, Chengdu, Sichuan, China 610041

^{||}GlaxoSmithKline, Medicines Research Centre, Gunnels Wood Road, Stevenage, SG1 2NY, U.K.

S Supporting Information



ABSTRACT: A novel molecular scaffold has been synthesized, and its incorporation into new analogues of biologically active molecules across multiple target classes will be discussed. In these studies, we have shown use of the tricyclic scaffold to synthesize potent inhibitors of the serine peptidase DPP-4, antagonists of the CCR5 receptor, and highly potent and selective PI3K δ isoform inhibitors. We also describe the predicted physicochemical properties of the resulting inhibitors and conclude that the tractable molecular scaffold could have potential application in future drug discovery programs.

INTRODUCTION

The search for new molecular scaffolds, amenable to expansion by parallel synthesis techniques, is an important challenge for synthetic medicinal chemists.¹ From our ongoing studies,^{2–4} into designing such scaffolds,^{5–8} we were drawn to the possibility of generating a series of readily functionalized compounds with well-defined conformations that provide points of diversity expansion for parallel substitution methods. Central to our scaffold design strategy was the growing evidence that nitrogen containing saturated heterocycles, fused to substituted heterocyclic rings, are present in many druglike molecules.^{9–12} In our design strategy, we wanted to combine this growing privileged motif within a tricyclic ring system containing a substituted 1,2,4-triazole ring. This would allow us to examine geometric isomerism (*cis*- and *trans*-ring fusion), the dihedral angle of the ring junction, and the influence of absolute chirality on biological activity. We therefore considered that the substituted tricyclic ring systems would

be ideal candidates to synthesize and evaluate across multiple biological targets (Figure 1).

In order to assess the utility of the tricyclic ring system as a new privileged scaffold, we were drawn to the exciting possibility of substituting the tricyclic scaffold into known biologically active compounds to compare both the resulting pharmacological activity and their predicted physicochemical parameters. From the outset of the project, we were interested in designing a novel molecular entity that, when appropriately functionalized, would possess potent activity and robust structure activity relationships (SARs) without being promiscuous.¹³ In addition, we wanted the new compounds to be “druglike” with respect to their predicted physicochemical properties.^{1,14–16} In order to test our hypothesis, we examined drug case histories where X-ray structural information was available to allow molecular docking experiments to guide our

Received: December 12, 2016

Published: January 27, 2017

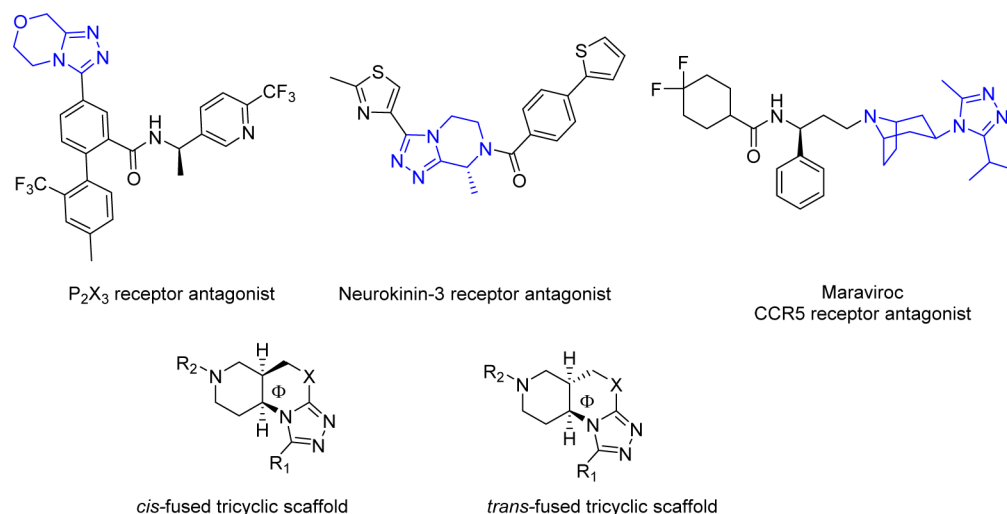


Figure 1. Molecular scaffolds amenable to further substitution. R_1 and R_2 are points of diversity expansion, $X = (-CH_2)_n$, where $n = 0$ to 2. Φ = the dihedral angle between the piperidine and substituted 1,2,4-triazole.

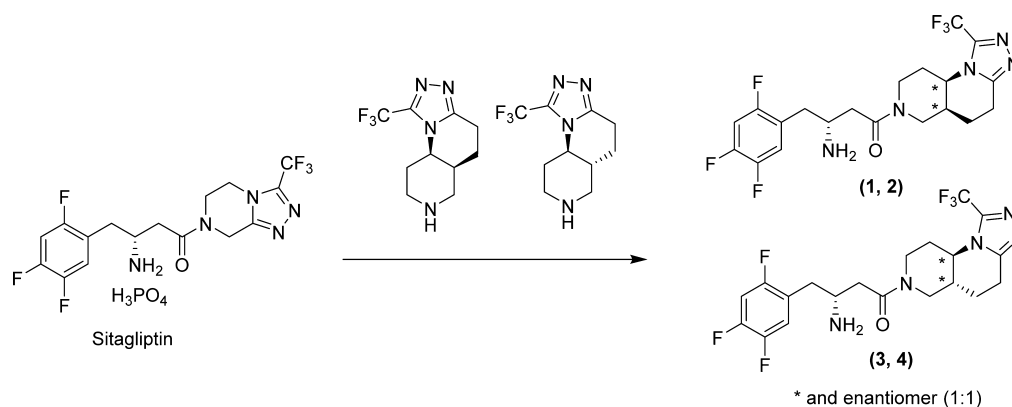


Figure 2. DPP-4 inhibitors (1–4), existing as a 1:1 mixture of either *cis*- or *trans*-diastereoisomers.

design strategies. As an outcome, we chose to incorporate the scaffold into three distinct series of compounds targeting; a serine protease (dipeptidyl peptidase-4, DPP-4), a G protein-coupled receptor (CCR5 receptor antagonist), and a kinase inhibitor (phosphoinositide 3-kinase, PI3K δ). We report here our initial findings in this area of privileged scaffold design, demonstrating potent cross-target biological activity of the resulting functionalized compounds combined with excellent predicted physicochemical properties.

RESULTS AND DISCUSSION

We recently communicated the synthesis and evaluation of new DPP-4 inhibitors based on the tricyclic scaffold,¹⁷ and we now report further structure activity relationships (SARs) of this interesting new class of potent DPP-4 inhibitors, demonstrating the utility for incorporation into druglike molecules (Figure 2).

Type-2 diabetes is a chronic disease, characterized by elevated blood sugar levels, leading to severe vascular complications and an increased mortality risk, and it is now well recognized that inhibition of the widely distributed serine protease dipeptidyl peptidase-4 (DPP-4) is a clinically validated target for antidiabetic therapy.¹⁸ Sitagliptin was the first approved DPP-4 inhibitor launched by Merck in 2006,¹⁹ and this was followed recently by omarigliptin,²⁰ a once weekly treatment for type-2 diabetes. Most recently, several series of structurally diverse DPP-4 inhibitors have been communicated

demonstrating that the search for new compounds is still an important goal for both pharmaceutical companies and academic groups (Figure 3).^{21–23}

We previously demonstrated that *cis*-fused diastereoisomers (1, 2) were more potent inhibitors than the corresponding *trans*-fused diastereoisomers (3, 4). A preference was observed

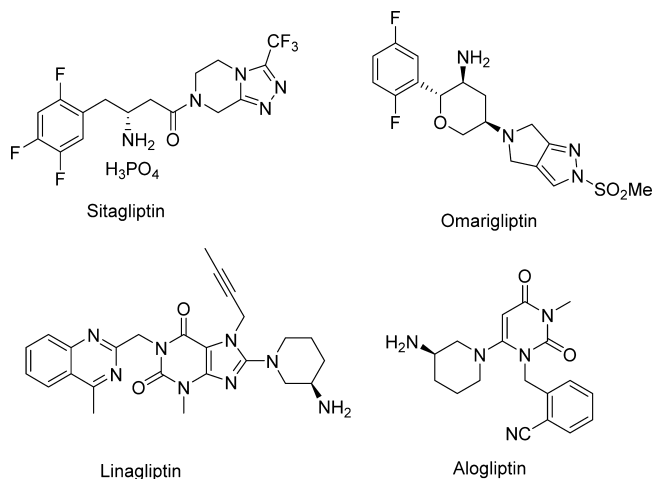
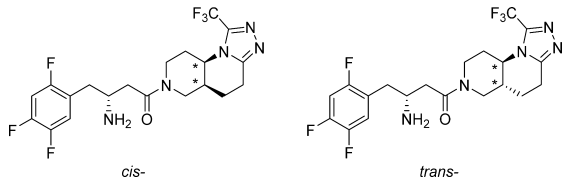


Figure 3. Selection of approved and late stage DPP-4 inhibitors.

for one of the resolved *cis*-diastereoisomers, although at the time of initial disclosure we could not determine the absolute chirality of the *cis*- enantiomer (Table 1).

Table 1. DPP-4 Inhibitory Activity^a



Compound ^b	<i>cis</i> - or <i>trans</i> -	DPP-4 IC ₅₀ [nM]
1	<i>cis</i> -	28 ± 1 ^c
2	<i>cis</i> -	70 ± 2 ^c
3	<i>trans</i> -	145 ± 5 ^c
4	<i>trans</i> -	537 ± 23 ^c

^aSitagliptin IC₅₀ 22 ± 2 nM. ^bSingle diastereomer with unknown absolute configuration. ^cPotency is given as IC₅₀ values (*n* = 2).

To determine the absolute stereochemistry of the resolved diastereoisomers (1 and 2), we embarked on a diastereomeric synthesis, as we were unable to obtain crystals of sufficient quality for single crystal X-ray structural analysis. Catalano et al. recently published²⁴ the stereoselective synthesis of 1-substituted cyclic ketone 7 using the stereoselective reduction of imine 6 generated from (*S*)-1-(4-methoxyphenyl)ethan-1-amine and δ keto ester 5 (Scheme 1).

Following literature precedent, we attempted to generate imine 9 from reaction of (*S*)-1-(4-methoxyphenyl)ethan-1-amine and δ keto ester 8. However, we were unable to generate the resulting imine even after heating under Dean–Stark conditions for several days. We therefore opted for the more routine reductive amination reaction stirring (*S*)-1-(4-methoxyphenyl)ethan-1-amine and δ keto ester 8 in 1,2-dichloroethane in the presence of sodium triacetoxy borohydride.²⁵ From the literature precedent, we predicted that the reductive amination using (*S*)-1-(4-methoxyphenyl) ethan-1-amine would generate diastereoisomer 2, which had previously been predicted through molecular docking to be the less-active diastereoisomer.^{17,26} The reductive amination reaction proceeded to afford 10 in 20% yield. Catalytic transfer hydrogenation removed the 4-methoxybenzyl group, affording the cyclized bicyclic lactam 11, as a separable 5:1 mixture of *cis*- to *trans*-isomers. The *cis*-fused isomer 11 was converted to thiolactam 12 through treatment with Lawesson's reagent. The thiolactam 12 was converted into the corresponding

tricyclic triazole 13 by refluxing in toluene with 2,2,2-trifluoroacetylhydrazide. The carbamate protecting group was removed to afford the key molecular scaffold 14, which was reacted with (*R*)-3-((*tert*-butoxycarbonyl)amino)-4-(2,4,5-trifluorophenyl)butanoic acid to generate 2, after removal of the protecting group (Scheme 2).

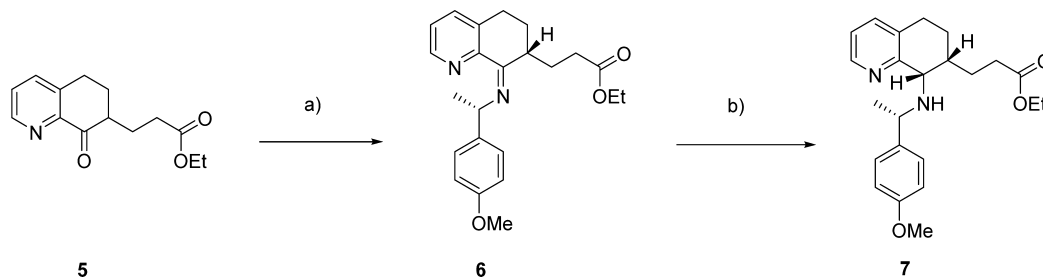
The final product (containing a mixture of 1 and 2) was analyzed by chiral HPLC, which showed two isomers: 2 (93%) and 1 (7%). From the literature precedent, we concluded that the stereoselective synthesis had generated the less biologically active diastereoisomer (Figure 4), thus demonstrating that the enantiomer was most likely isomer 1? However, further detailed work needs to be undertaken to demonstrate the precedent-based assignment of stereochemistry, and this work will be reported in due course.

To understand the observed differences seen in DPP-4 inhibitory activity for the isomers, docking studies were carried out with the crystal structure of sitagliptin in DPP-4 (PDB code 1X70).^{19,26} It has been known that the primary amine present in sitagliptin has strong ionic interactions with E₂₀₅, E₂₀₆, and Y₆₆₂ and π -stacking with Y₆₆₂—all of which have been shown to be conserved within the compounds (1, 2). In addition, sitagliptin has further electrostatic and van der Waals interactions with S₂₀₇, F₃₅₇, and R₃₅₈ in the S2 pocket and a further hydrogen bonding interaction, through a water molecule, to Y₅₄₇ (Figure 5a).¹⁹ From the molecular docking experiments, it was shown that the more active *cis*-fused diastereoisomer 1 maintained the strong interactions with S₂₀₇, F₃₅₇, and R₃₅₈ but had suboptimal hydrogen bonding interaction with Y₅₄₇ (Figure 5b). This might explain the small reduction in activity of 1 when compared to sitagliptin. Similarly, 2 was shown to lack the hydrogen bonding interactions with Y₅₄₇, S₂₀₇, and R₃₅₈ (Figure 4c), suggesting a likely rationale for the observed differences seen in DPP-4 inhibitory activity between 1 and 2.

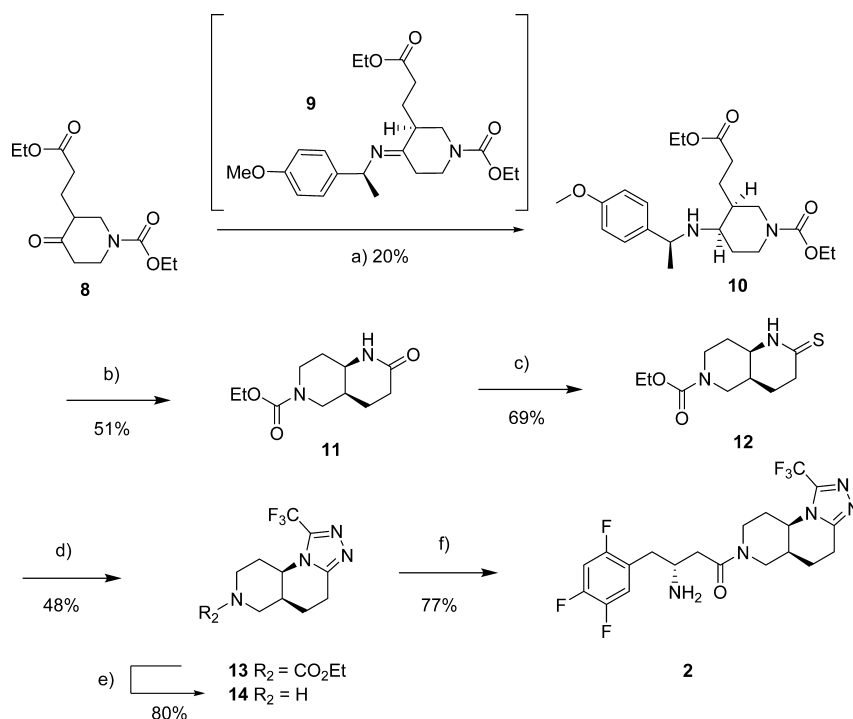
Due to the convergent synthesis, it was possible to rapidly synthesize a range of analogs (40–47) which were prepared in a similar fashion to those already reported (1–4) (Scheme 3).

The known bicyclic thioamides (15, 16)^{17,27} were reacted with a range of substituted acyl hydrazides (R₁CONHNH₂) to give tricyclic triazoles (17–23), which were deprotected to the corresponding N–H piperidines (24–31) in refluxing KOH in aqueous ethanol. The resulting piperidines (24–31) were reacted with (*R*)-3-((*tert*-butoxycarbonyl)amino)-4-(2,4,5-trifluorophenyl)butanoic acid to give, after deprotection, the corresponding analogs (40–47).

Scheme 1. Catalano et al. Synthetic Procedure^a



^aReagents and conditions: (a) (*S*)-1-[4-(methoxy)phenyl]ethanamine, *p*-TosOH, toluene, Dean–Stark, 4 h.; (b) NaBH(OAc)₃, 1,2-DCE, 16 h (61%).

Scheme 2. Synthesis of **2** Derived from (*S*)-1-(4-Methoxyphenyl)ethan-1-amine and δ Keto Ester **8**^a

^aReagents and conditions: (a) (*S*)-1-(4-methoxyphenyl)ethan-1-amine, sodium triacetoxo borohydride, 1,2-dichloromethane rt 20 h; (b) ammonium formate, ethanol, 10% Pd on C, 70 °C, 10 h; (c) Lawesson's reagent (0.5 equiv), 120 °C, toluene, 30 min; (d) CF₃CONHNH₂, toluene 120 °C, 20 h; (e) KOH, water/ethanol, 120 °C, 20 h; (f) (i) EDCI, HOBt, DMF, (*R*)-3-((*tert*-butoxycarbonyl)amino)-4-(2,4,5-trifluorophenyl)butanoic acid, rt, 20 h, (ii) 4 N HCl in 1,4-dioxane.

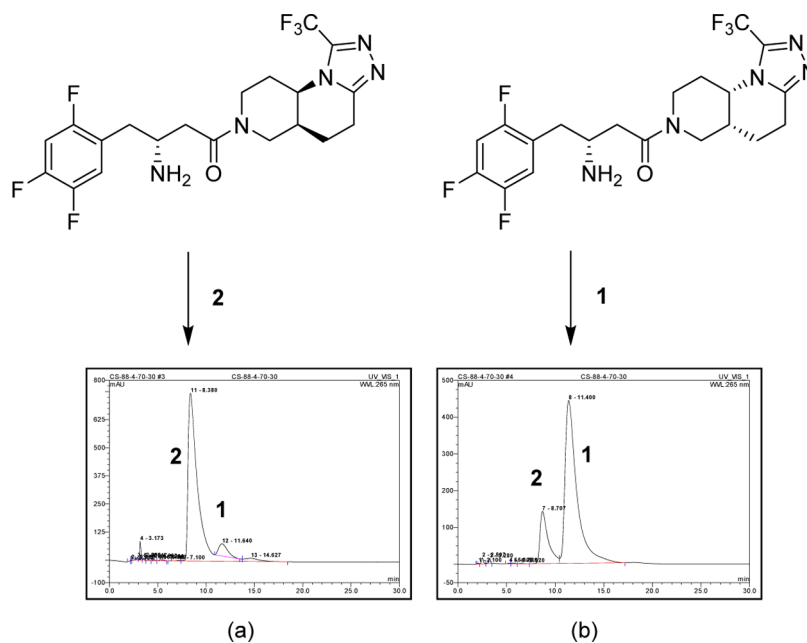


Figure 4. (a) Analytical chiral HPLC analysis of the final mixture of products, containing **2** (93%) and **1** (7%); (b) sample spiked with the previously separated, enantiomer **1**. Phenomenex LC Lux 5u Amylose-2 packed column (250 × 4.6 mm) at a flow rate of 1.5 mL/min, using 70% hexane: 30% ethanol supplemented with 0.2% diethylamine over 30 min.

Through substituting the group R₁, an interesting structure activity relationship (SAR) was revealed within this class of new DPP-4 inhibitors (Table 2).

Once more, the *cis*-fused diastereoisomer **41** proved more active than the *trans*-fused diastereoisomer **47**. It is encouraging to note that R₁ substitution, with either small alkyl groups (**40**,

41) or heterocycles (**44–46**), gave compounds with high DPP-4 inhibitory activity, while larger groups (**42**, **43**) led to a reduction in DPP-4 inhibitory activity. This suggested a steric requirement for the R₁ substituent within the DPP-4 active site. This is most notable when considering the 3-ethoxy-pyrid-2-yl **43** and 2-pyridyl **44** analogues, which shows that an increase in

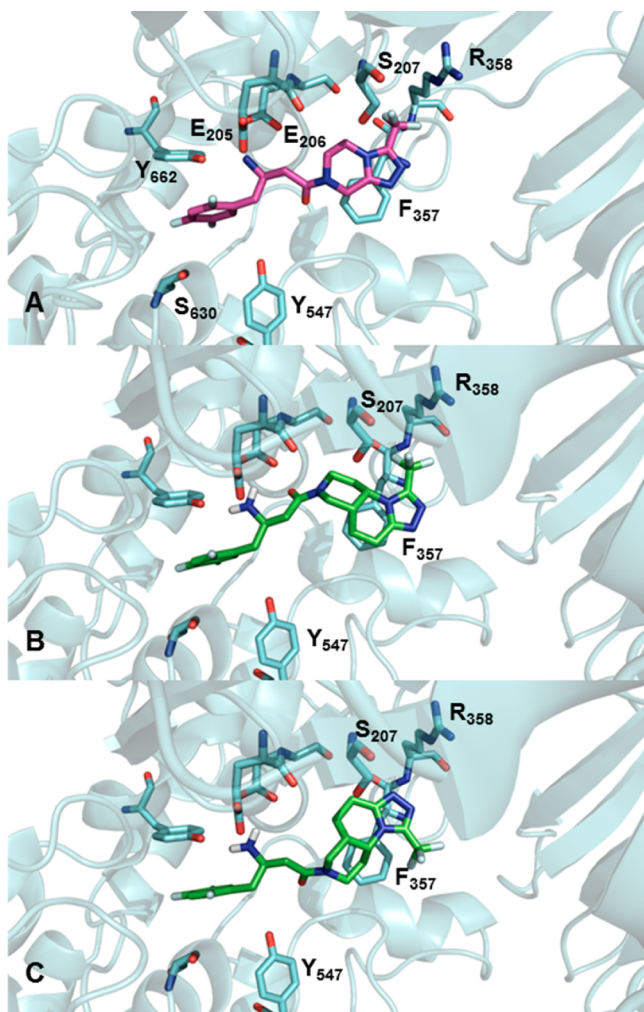


Figure 5. (a) Sitagliptin (magenta) in DPP-4 (PDB code 1X70); (b) eutomer **1** docked into DPP-4; (c) diastereoisomer **2** docked into DPP-4.²⁶

size results in a 3-fold reduction in DPP-4 inhibitory activity. This can be rationalized through considering the docking of **43**, which showed a possible steric clash of the ethoxyl group with S₂₀₉ in the active site (Figure 6).²⁶

One of our success criteria was that the resulting compounds should be lead-like with respect to their physicochemical properties.^{15,16,28} As a metric to demonstrate lead-likeness, we chose to evaluate the lipophilic ligand efficiency (LIFE)^{11,29–31} of our most potent analogues and compare them to sitagliptin (Table 3).

It was gratifying to note that **40** displayed very good predicted druglike characteristics (LIFE 6.9), comparing favorably to sitagliptin. Further analysis showed **40** to have a favorable topological polar surface area (TPSA)³³ value of 77 Å² and high predicted solubility in water (calculated solubility at pH 7.4: 5.39 mg/mL, sitagliptin: 3.20 mg/mL).³²

Having demonstrated that the molecular scaffold was capable of generating compounds with excellent biological activity balanced with good calculated lead-like physicochemical properties against one target class, we chose to look at designing a series of GPCR receptor antagonists. In our second case study, we chose the chemokine receptor CCR5 as the biological target, as we were drawn to the structural similarity

between the tricyclic ring system and the corresponding group present in the CCR5 receptor antagonist, maraviroc (Figure 7).

The CCR5 receptor is a chemokine receptor, which is located on the cell surface of T cells and can bind specific peptide ligands called chemokines and belong to a large family of the seven transmembrane GPCRs. The human CCR5 receptor itself is a 352 amino acid protein and consists of seven transmembrane spanning helices connected through three extracellular loops (ECL1, ECL2, and ECL3), three intracellular loops, an extracellular N-terminus, and an intracellular C-terminus and N-terminus functionality. The extracellular loops and transmembrane helices are responsible for binding ligands, and the intracellular regions are responsible for signal transduction. The activation of the chemokine receptor CCR5 through its binding of endogenously expressed chemokines (macrophage inflammatory proteins MIP-1 α and MIP-1 β as well as “regulated on activation, normal T cell expressed, and secreted” RANTES) can cause typical cellular responses, including inhibition of cAMP production or stimulation of intracellular Ca²⁺.³⁴ CCR5 is a coreceptor for HIV entry into T cells, and maraviroc is the only marketed CCR5 receptor antagonist for R5 HIV therapy to date.^{35,36}

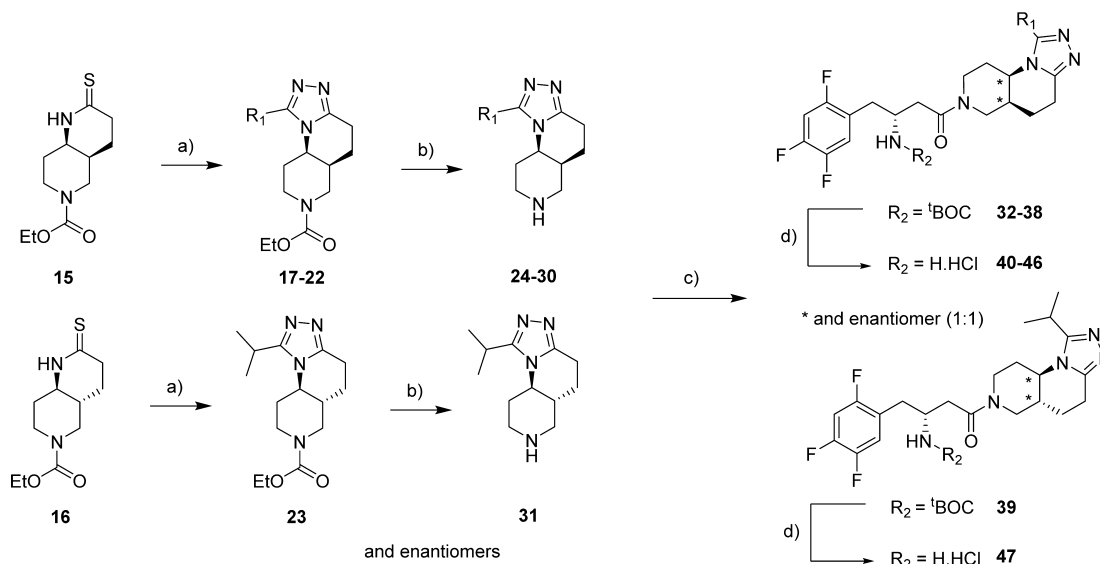
While our chemical design appears a rational “fast-follower” process, we were concerned that the tropane ring present in maraviroc had been shown to give a 40-fold increase in affinity compared to the piperidine analogue.³⁷ In addition, the triazole group in maraviroc adopts a conformation where it is orthogonal to the tropane ring, whereas in our proposed analogue the triazole group would be occupying a different spatial configuration. As a consequence of these considerations, we decided to generate a receptor model based on the reported maraviroc-bound X-ray crystal structure of CCR5 and examined the overlay and key receptor interactions of our proposed analogues to that of maraviroc (Figure 8).²⁶ In the molecular docking, it was shown that a very good overlay to maraviroc was observed with the *cis*-fused diastereoisomer **48**. In addition, key hydrogen bonding interactions were seen to T₁₉₅, T₂₅₉, Y₂₅₁, E₂₈₃, and Y₃₇ and strong face-to-face interaction with W₈₆ interactions was reported for maraviroc.³⁸

In light of the positive docking results, we proceeded to embark on a synthesis of the maraviroc analogues, using an analogous route to the previously reported synthesis (Scheme 4). Unfortunately, the final compounds could not be separated into single diastereoisomers, and so the compounds were screened as either a mixture or separated *cis*- or *trans*-diastereoisomers (**48–49**).

Benzyl (*S*)-(3-oxo-1-phenylpropyl)carbamate³⁹ was reacted with piperidines (**24**, **50**) under reductive amination conditions²⁵ to give Cbz-protected intermediates (**51a–b**) which were deprotected and acylated with 4,4-difluorocyclohexane-1-carboxylic acid to generate the maraviroc analogues (**48**, **49**) in good overall yield.

RANTES was chosen as the agonist in our biological evaluation, as receptor agonism with MIP-1 α was shown to be less reproducible in our hands. This biological screen was carried out using the Ca²⁺ signaling assay by testing the ability of a single concentration of antagonist [30 nM (**48**) or 1 μ M (**49**), final concentration] to shift agonist (RANTES) concentration response curves, and the estimated affinity values (pK_D)⁴⁰ are summarized in Table 4.

It is interesting to note that, even though the lipophilic tropane interaction present in maraviroc was absent in **48**, a very good level of CCR5 receptor antagonism was observed.

Scheme 3. Synthetic Route to Compounds 40–47^a

^aReagents and conditions: (a) $R_1\text{CONHNH}_2$, toluene 120 °C, 20 h. 31–75% yields. (b) KOH, water/ethanol, 120 °C, 20 h. 54–87% yields. (c) EDCI, HOBT, DMF, (*R*)-3-((*tert*-butoxycarbonyl)amino)-4-(2,4,5-trifluorophenyl)butanoic acid rt, 20 h, 45–98% yields. (d) 4 N HCl in dioxane, 95–100% yields. Compounds 40–47 exist as a 1:1 racemic mixture of either *cis*- or *trans*-diastereoisomers.

Table 2. DPP-4 Inhibitory Activity^a

Compound ^b	<i>cis</i> - or <i>trans</i> -	R_1	DPP-4 IC_{50} [nM] ^c
40	<i>cis</i> -	CH ₃	28 ± 0.9
41	<i>cis</i> -	isopropyl	31.8 ± 0.8
42	<i>cis</i> -	benzyl	123.3 ± 6.8
43	<i>cis</i> -	6-ethoxypyrid-2-yl	139 ± 4.1
44	<i>cis</i> -	2-pyridyl	43.4 ± 1.3
45	<i>cis</i> -	2-pyrazinyl	60.0 ± 2.1
46	<i>cis</i> -	4-(2-methyl)thiazolyl	50.2 ± 1.0
47	<i>trans</i> -	isopropyl	151.7 ± 9.4

^aSitagliptin IC_{50} = 22 ± 2 nM (n = 16). ^b1:1 mixture of diastereoisomers. ^cPotency is given as IC_{50} values (n = 2).

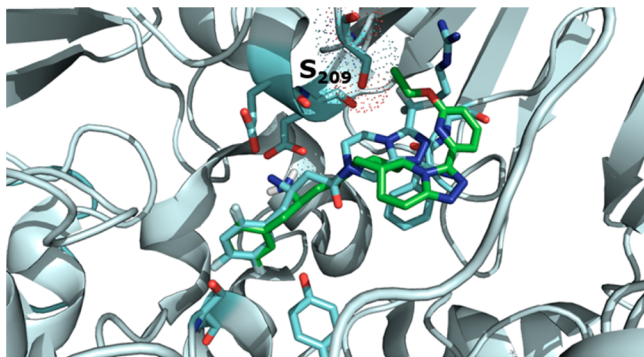


Figure 6. Proposed binding of 43 in the DPP-4 active site (PDB code 1X70) overlaid on sitagliptin (cyan), showing a steric clash with S₂₀₉.²⁶

Importantly, a reduction in calculated lipophilicity and molecular weight might lead to an improvement in ADME

Table 3. Calculated Physicochemical Parameters of Sitagliptin and Compounds 1, 40, and 41

Compound	pIC ₅₀	cLogP ^a	cLogD ^a	MWt	LIPE ^b
Sitagliptin	7.66	1.26	−0.01	407.3	6.4
1	7.56	1.84	0.44	461.5	5.7
40	7.56	0.7	−0.07	407.5	6.9
41	7.49	1.95	0.55	435.5	5.6

^aCalculated using instant JChem.³² ^bLIPE = pIC₅₀ − cLogP.

properties? However, further research is required to demonstrate that the calculated druglike properties may lead to an improved over all profile.

Having demonstrated that the new molecular scaffold was capable of generating compounds with excellent biological activity and activity against two target classes, we chose to look at utilizing the scaffold into the design of a series of kinase inhibitors. In this approach, we wanted to use the molecular scaffold to function as a key molecular recognition group to increase kinase activity and also fine-tune kinase isoform selectivity. In this respect, we were drawn to the exciting possibility of designing a set of potent and selective phosphoinositol-3 kinase δ isoform inhibitors, an area of interest from our University of Nottingham and GlaxoSmithKline research teaching collaboration.⁴¹

Phosphoinositol-3 kinase (PI3K) signaling plays a central role in cellular functioning, including growth, proliferation, survival, or migration. It therefore has a pivotal role in diseases such as those related to the respiratory tract, e.g. asthma⁴² and cancer.⁴³ These lipid kinases catalyze phosphorylation, which leads to the production of phosphatidylinositol (PI(3,4,5)P₃) through the isoforms α , β , γ , and δ . (PI(3,4,5)P₃) is involved in the signaling of kinase Akt (protein kinase B), which is a serine/threonine protease involved in cell growth, survival, proliferation, and angiogenesis. Phosphoinositol (3,4,5)-triphosphate (PIP₃) is an important intracellular second messenger, whose biological action occurs through stimulating increase of the intracellular calcium ion concentration. The PI3

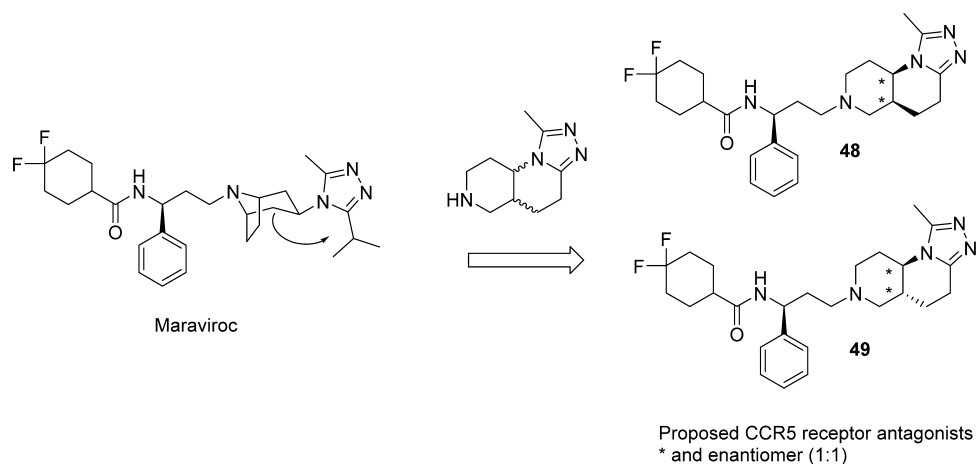


Figure 7. Proposed new CCR5 receptor antagonists (48 and 49) based on maraviroc.

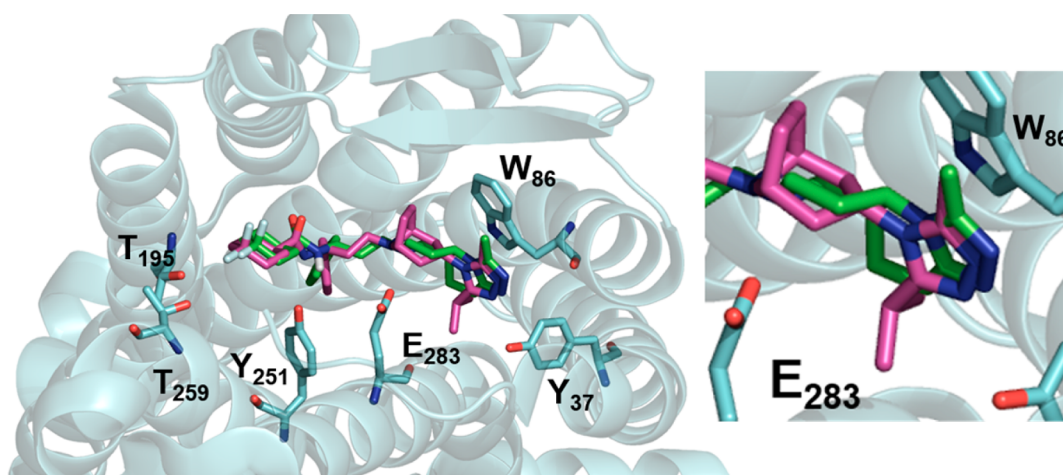
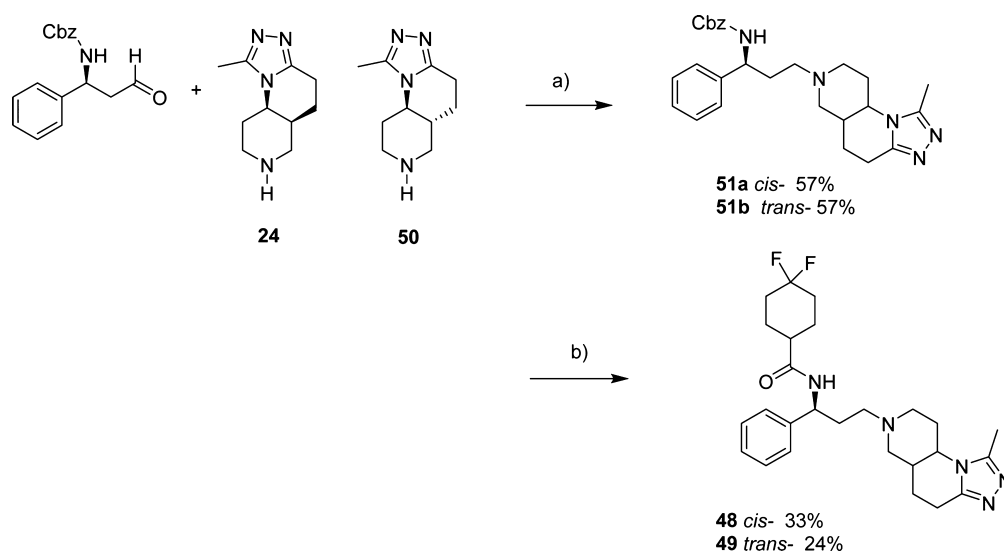


Figure 8. Maraviroc (magenta) and *cis*-fused diastereoisomer 48 (green) docked into the CCR5 receptor model (generated from PDB code 4MBS). Illustrated H-bond and lipophilic interactions shown with CCR5 amino acid residues. Close up showing the overlay of the tropane and 1,2,4-triazole groups.

Scheme 4. Synthetic Route to Compounds 48–49^a



^aReagents and conditions: (a) NaBH(OAc)₃, DCE, rt, 20 h. (b) (i) Pd/C, MeOH, hydrogen, rt, 20 h; (ii) 4,4-difluorocyclohexane-1-carboxylic acid, HATU, DIPEA, DMF, rt, 20 h. n.b. yields of final products are quoted after reverse phase HPLC purification.

Table 4. pK_D and Key Predicted Physicochemical Values of 48 and 49 Compared to Maraviroc

Compound	pK_D^a	$cLogP^b$	$cLogD^b$	MWt	LIPE
maraviroc	8.8 ± 0.2	3.6	1.4	514	5.2
48	8.0 ± 0.2	2.1	0.2	472	5.9
49	6.5 ± 0.1	2.1	0.2	472	4.4

^aThe estimated affinity value for each antagonist (pK_D) was calculated from the shift of the agonist dose response curve brought about by addition of a single concentration of antagonist using the Gaddum equation. Tested $n = 6$. ^bCalculated using Instant JChem³²

kinase family can be divided into three different classes depending on their domain structure. The main focus in current research is on the class 1 PI3Ks, which consist of four members. The majority of research is concentrated on the class 1A subunit isoforms PI3K α , PI3K β , and PI3K δ , and furthermore the class 1B subunit PI3K γ . Due to their fundamental roles, the design of selective inhibitors is important to consider, as nonselective compounds could result in toxicity. As PI3K δ expression is limited to leukocytes, its inhibition has potential for the treatment of respiratory diseases⁴² and leukemia.^{44,45} The reduction of response in PI3K δ knock in (KI) mice and animals was seen after treatment with a PI3K δ specific inhibitor, which is demonstrated by reduced clonal expansion of CD4 cells and diminished pathology in asthma models.⁴⁶ The inactivation of PI3K δ also affects mast cell function, which plays an important role in allergic responses and asthma.

In this case study, we considered pictilisib,⁴⁷ a pan PI3K inhibitor, as the chemical starting point, as the X-ray crystal structure was available.⁴⁸ In addition, 52 was recently reported as a more selective PI3K δ inhibitor [PI3K α (340-fold), PI3K β (200-fold), PI3K γ (410-fold)], suggesting that PI3K δ isoform selectivity could be achieved within the thienyl pyrimidine class

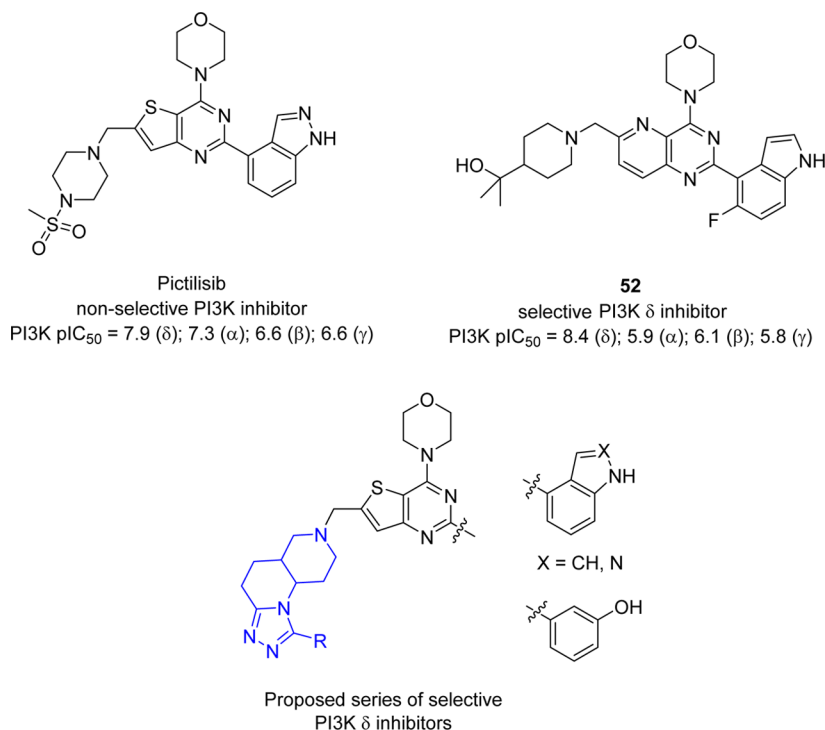
of PI3K inhibitors.⁴⁹ Our plan was to investigate the role for the incorporation of the molecular scaffold to synthesize a series of potent and selective PI3K δ inhibitors (Figure 9).

Modest PI3K δ isoform selectivity has been reported though an edge to face interaction of the thienyl pyrimidine with W_{760} —the so-called tryptophan shelf interaction.⁴⁹ In addition, it is known that, even though there is good homology between the PI3K isoforms, an important residue change exists between the four isoforms that might also aid δ isoform selectivity. An overlay of the available crystal structures reveals a potential key π -cation interaction present in the structures of the α (K_{750}), β (K_{771}), and γ (K_{771}) isoforms with W_{760} (δ -numbering) that is not present in PI3K δ (T_{750}). This led us to the exciting possibility that our inhibitors might be able to form an extra van der Waal π - π face to face interaction with W_{760} , an interaction occluded in the case of the other isoforms (Figure 10).

Furthermore, it has been reported that selectivity for PI3K δ can be achieved in part due to the effect of the affinity pocket group R_2 , with $R_2 = 4$ -substituted indole giving rise to good PI3K δ isoform selectivity.⁴⁹ We therefore decided to use a small 3D matrix-based approach (18 compounds) to evaluate the potency and selectivity profiles of substituting groups R_1 , R_2 , and R_3 (Figure 11). In addition, we included the open chain analogues (62–67) to evaluate the role of the tricyclic ring system on potency and selectivity.

The synthesis of the compounds (62–79) was accomplished through a two-step procedure. The acyclic intermediates (53 and 54) were prepared by the high-yielding 1,2,4-triazole synthesis method as outlined by Stocks (Scheme 5).⁴

The six substituted piperidines (groups R_1 in Figure 11) were reacted with aldehyde 55⁴⁷ using picoline borane⁵¹ as the reducing agent in 10% acetic acid in methanol to generate the key intermediates (56–61) that were then subjected to Suzuki–Miyaura cross-coupling reactions^{52,53} to afford compounds (62–79) in high yield (Scheme 6).

**Figure 9.** Potent pan PI3K inhibitor pictilisib, δ -selective PI3K inhibitor 52, and proposed inhibitors based on the tricyclic scaffold.

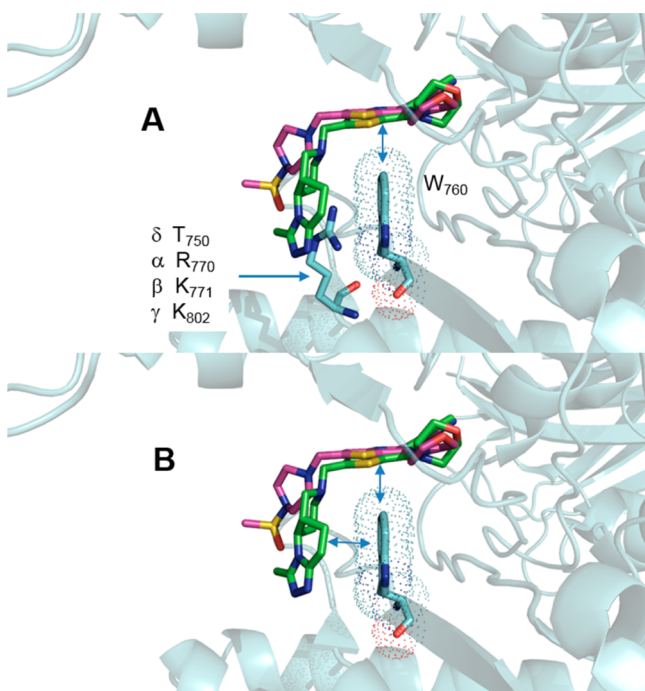


Figure 10. (A) Depiction of the tryptophan shelf and amino acid changes in PI3K isoforms to occlude binding of the tricyclic scaffold—shown with PI3K α isoform—pdb 5DXT.⁵⁰ (B) Molecular docking of *cis*-fused diastereoisomer 73 into PI3K δ (pdb 2WXP⁴⁸), highlighting potential face-to-face interaction with the tricyclic scaffold. Pictilisib (magenta) and 73 (green).

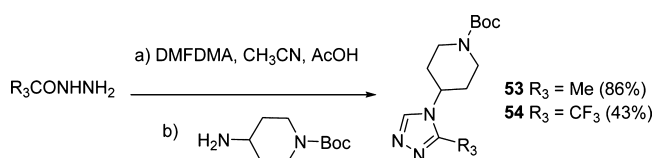
The compounds were screened against PI3K isoforms, and their biological activities are reported in Table 5.⁵⁴

It is interesting to note that all the compounds demonstrated a good degree of isoform selectivity for PI3K δ over PI3K α , PI3K β , and PI3K γ . However, the following discussion will concentrate on the PI3K δ/α isoform selectivity (Figure 12).

A plot of PI3K δ potency versus PI3K α potency showed a general trend that compounds with $R_2 = 4$ -substituted indolyl [e.g., 73 (~4000-fold), 72, and 78 (~2000-fold)] were more PI3K δ isoform selective⁴⁹ (Figure 13).

It is noteworthy that high PI3K isoform selectivity was also achieved, where $R_2 = 4$ -indazolyl (71, $\delta/\alpha \sim 500$ -fold, $\delta/\beta \sim 400$ -fold, $\delta/\gamma \sim 400$ -fold), demonstrating that high PI3K δ isoform potency, and therefore selectivity, could be enhanced by the methyl-substituted *cis*-fused tricyclic molecular scaffold

Scheme 5. Synthesis of Acyclic Analogue Intermediates (53–54)^{*}



^{*}The intermediates were deprotected with TFA in dichloromethane immediately prior to the subsequent reaction.

over the acyclic scaffold (compare 71 with 63), suggesting that our initial proposal from molecular docking studies for further interaction of the *cis*-fused tricyclic scaffold with W_{760} may be driving the PI3K δ isoform activity and therefore selectivity independently of the known activity pocket selectivity afforded by the 4-substituted indole group. Further analysis of the role of group R_1 showed a general trend, with the tricyclic compounds showing a greater level of activity at PI3K δ than PI3K α when compared to the acyclic compounds. This is very apparent when looking at a matched-pair analysis⁵⁵ between compounds containing the acyclic scaffold (groups A) and the *cis*-fused tricyclic containing compounds (groups B)—compare 65 with 69, 66 with 68, 63 with 71, 67 with 72, and 64 with 73. (Figure 14). From the analysis, the matched-pairs generally have similar levels of PI3K α activity, but the inclusion of the *cis*-fused tricyclic ring increases the level of PI3K δ activity, with the largest difference in PI3K δ activity being observed for the matched pairs (67 and 72).

A similar profile was observed between compounds containing the acyclic scaffold (groups A) and the *trans*-fused tricyclic containing compounds (groups C)—compare 65 with 75, 62 with 79, 66 with 74, 63 with 76, 67 with 77, and 64 with 78 (Figure 15).

Further examination of group R_1 as a function of PI3K δ/α selectivity showed that the tricyclic compounds (groups B and C) give rise to a very good selectivity profile with (72, 73, and 78), showing the optimal balance between very high PI3K δ activity and selectivity over PI3K α (Figure 16).

Indeed, it is very encouraging to note that compound 73 achieved a very high degree of PI3K δ selectivity over PI3K β (~400-fold) and PI3K γ (2000-fold). To test the druglikeness of the synthesized compounds, the physicochemical properties of 73 were calculated (PI3K δ (pIC₅₀ = 9.1), MWt 540.7, cLogP 3.9, clogD 2.5, TPSA 88 Å², solubility at pH 7.4 in water:

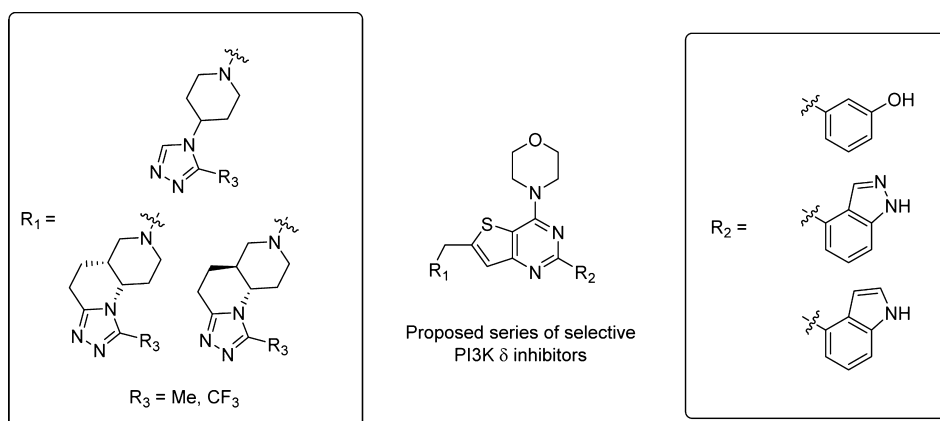
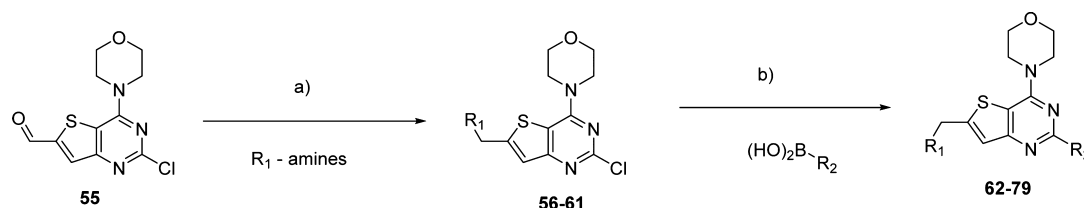
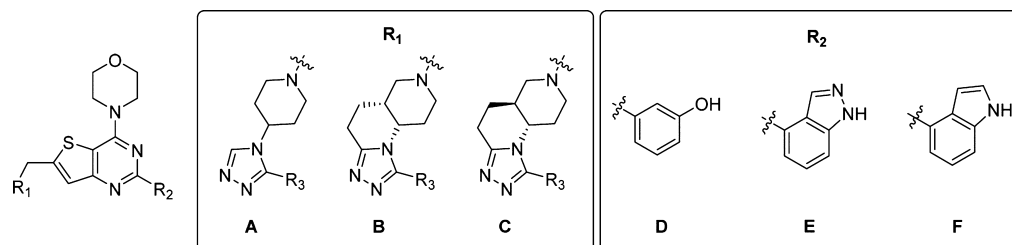


Figure 11. 3D-Matrix-based chemistry plan to explore PI3K δ isoform selectivity of the tricyclic molecular scaffold.

Scheme 6. Synthesis of Potential PI3K Inhibitors (62–79)^a

^aReagents and conditions: (a) picoline borane/10% AcOH in methanol 20 h, yields 30–91%; (b) Na₂CO₃, EtOH (aq), boronic acid (1.5 equiv), bis(triphenylphosphine) palladium chloride (0.1 equiv), microwave 120 °C, 30 min, yields 54–97%. Compounds 68–79 exist as a 1:1 racemic mixture of either *cis*- or *trans*- diastereoisomers.

Table 5. Biological Evaluation and Isoform Selectivity for PI3K δ for Compounds 62–79

Example	R ₁	R ₂	R ₃	Isoform potency ^{a,b} (pIC ₅₀)				Isoform selectivity		
				PI3K δ	PI3K α	PI3K β	PI3K γ	δ/α	δ/β	δ/γ
62	A	D	CH ₃	8.4 ± 0.0	7.0 ± 0.0	6.8 ± 0.1	6.7 ± 0.1	25	40	50
63	A	E	CH ₃	8.0 ± 0.0	6.5 ± 0.1	6.0 ± 0.2	6.0 ± 0.0	32	100	100
64	A	F	CH ₃	8.4 ± 0.1	5.7 ± 0.2	6.4 ± 0.0	5.7 ± 0.2	501	100	501
65	A	D	CF ₃	8.6 ± 0.2	7.2 ± 0.0	7.0 ± 0.0	6.8 ± 0.0	25	40	63
66	A	E	CF ₃	7.7 ± 0.0	6.5 ± 0.1	5.9 ± 0.2	6.1 ± 0.0	16	63	40
67	A	F	CF ₃	7.7 ± 0.1	5.4 ± 0.0	6.1 ± 0.2	5.5 ± 0.0	200	40	158
68	B	E	CF ₃	8.6 ± 0.0	6.5 ± 0.0	6.4 ± 0.0	6.1 ± 0.0	126	158	316
69	B	D	CF ₃	9.2 ± 0.0	7.2 ± 0.0	7.3 ± 0.0	6.8 ± 0.0	100	79	251
70	B	D	CH ₃	*	*	*	*	*	*	*
71	B	E	CH ₃	8.5 ± 0.4	5.8 ± 0.3	5.9 ± 0.3	5.9 ± 0.2	501	398	398
72	B	F	CF ₃	9.1 ± 0.1	5.8 ± 0.1	7.0 ± 0.1	6.2 ± 0.1	1995	126	794
73	B	F	CH ₃	9.1 ± 0.0	5.5 ± 0.1	6.5 ± 0.2	5.8 ± 0.0	3981	398	1995
74	C	E	CF ₃	8.1 ± 0.0	6.8 ± 0.0	6.2 ± 0.0	6.0 ± 0.0	20	79	126
75	C	D	CF ₃	9.0 ± 0.3	7.5 ± 0.1	7.3 ± 0.1	6.7 ± 0.0	32	50	200
76	C	E	CH ₃	8.4 ± 0.1	6.8 ± 0.2	6.3 ± 0.1	6.5 ± 0.1	40	126	79
77	C	F	CF ₃	8.8 ± 0.2	6.3 ± 0.1	6.8 ± 0.2	6.4 ± 0.2	316	100	251
78	C	F	CH ₃	9.0 ± 0.0	5.7 ± 0.1	6.5 ± 0.2	6.1 ± 0.2	1995	316	794
79	C	D	CH ₃	9.1 ± 0.4	7.0 ± 0.1	6.9 ± 0.1	6.3 ± 0.3	126	158	631

^aPotency against the different PI3K isoforms is given as pIC₅₀ values ($n = 2$). ^bThe potency threshold for the PI3K δ assay is \sim pIC₅₀ 9 due to substrate concentration. *Example 70 proved insoluble in the assay buffer for biological testing.

0.02 mg/mL, solubility category: Low, LIPE = 5.2).³² While the properties may not be ideal for oral druglikeness, the compounds may fulfill inhalation delivery criteria, where MWt appears to be less important for successful drug development.^{46,56} In addition, the compound may well prove very useful as a highly selective tool compound to further probe biological mechanisms for the role of PI3K δ in other therapies.^{57–59}

Within the three case histories presented, the *cis*-fused diastereoisomer of the tricyclic scaffold (Figure 1) proved the most potent diastereoisomer. It is interesting to speculate that a common molecular recognition motif might be present in each of the biological targets, and further work is ongoing in our laboratory to explore this exciting possibility.

Implicit to the design strategy was to generate a series of new molecular entities that could be readily diversified by robust

synthetic chemistry. In our considerations, it was important to ensure that the scaffolds contained sufficient functionality to allow hydrogen bonding interaction within diverse biological systems but also possessed a sufficient degree of lipophilicity to make interactions with lipophilic amino acids within the binding pockets. In our design phase, we rationalized that the optimal strategy for obtaining biological interactions in novel scaffolds was to separate the polar groups with hydrogen bond neutral linking groups and, importantly, to avoid the proximity of too many polar interactive groups that could lead to reduction in binding. We therefore suggest the following simple strategy to consider when generating new molecular scaffolds for high hit rate compound libraries, as well as for use in lead optimization programs where scaffold diversity is required:

- Examine the medicinal chemistry literature and identify core “over-represented” features in druglike molecules to

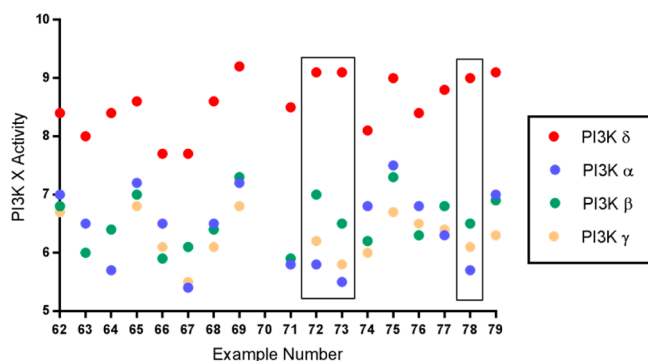


Figure 12. Plot of PI3K isoform activity versus example number demonstrating the general high level of PI3K δ isoform selectivity observed with all examples. Highlighted are key compounds 72, 73, and 78—compounds that show the most favorable PI3K δ isoform selectivity profile.

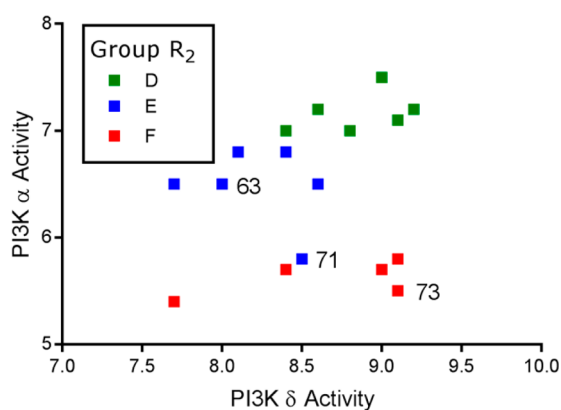


Figure 13. Plot of PI3K δ activity versus group PI3K α activity highlighting changes in group R₂ showing the high PI3K δ isoform selectivity imparted by the 4-substituted indole (group F).

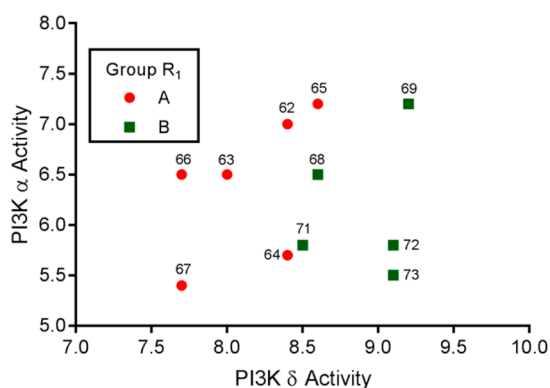


Figure 14. Matched-pair analysis for the acyclic scaffold containing compounds (groups A) and the *cis*-fused tricyclic containing scaffold (groups B) showing a general trend for an increase in PI3K δ isoform activity through the inclusion of the *cis*-fused tricyclic scaffold.

enable design mimics with structural diversity, while maintaining core physicochemical properties.

- Hypothesize new ring systems containing aspects of these features (i.e., fused/spirocyclic ring systems) containing a maximum of two points of diversity, remembering the virtue of rings within medicinal chemistry design has good precedence⁶⁰ due to their higher intrinsic ligand efficiency, increased crystallinity,

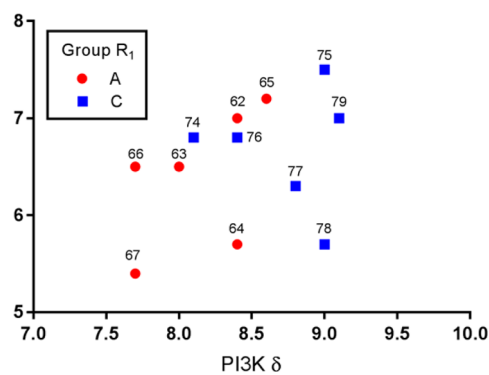


Figure 15. Matched-pair analysis for the acyclic scaffold containing compounds (groups A) and the *trans*-fused tricyclic containing scaffold (groups C) showing a general trend for an increase in PI3K δ isoform activity through the inclusion of the *trans*-fused tricyclic scaffold.

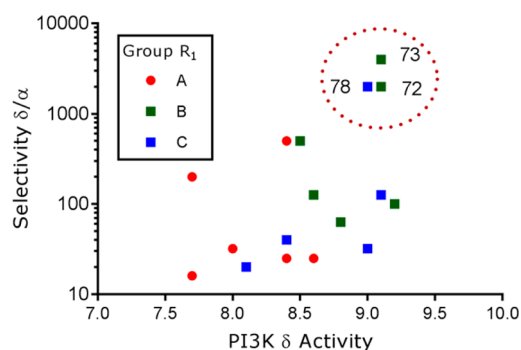


Figure 16. Plot of PI3K δ activity as a function of PI3K δ isoform selectivity (vs PI3K α), highlighting changes to group R₁.

and reduction in degrees of flexibility (ΔG vs ΔS) compared to acyclic systems.

- Re-evaluate chemical design to remove overcomplexity and unwanted functionality to improve synthetic tractability, including stereocontrol for chiral centers, and include “simple opportunities” to modify scaffolds at a later stage.⁶¹
- Enumerate and profile a small subset of the virtual library based on physicochemical properties and deselect scaffolds that do not offer compounds with good physicochemical properties.¹
- Generate sets of closely related scaffolds with common capping chemistries to expedite synthesis.
- Complete the library matrix to build SAR and discover serendipitous synergistic group effects.

CONCLUSION

In summary, we have shown the successful synthesis of promising new druglike compounds as inhibitors of DPP-4, antagonists of the CCR5 receptor, and highly selective and potent inhibitors of PI3K δ based on an interesting new molecular scaffold. Importantly, the compounds possess good predicted lead- or druglike properties,^{15,62,32} giving extra evidence for the scaffold to be considered privileged for medicinal chemistry projects. In the DPP-4 case study, we have shown the stereochemical preference for the *cis*-fused diastereoisomer of the octahydro[1,2,4]triazolo[4,3-*a*][1,6]-naphthyridine tricyclic ring system and have described initial studies toward a diastereoselective synthesis of the new

molecular scaffold resulting in determination of the absolute configuration of the eutomer. Further work is ongoing in our laboratories on the incorporation of the new molecular scaffold into new compounds to interact with biological targets, and these will be reported in due course.

EXPERIMENTAL SECTION

Chemistry—General Methods. All reactions with air- and humidity-sensitive reagents were carried out under an atmosphere of nitrogen. The flasks were flushed with nitrogen. The liquids were added using plastic syringes. All starting materials, reagents and solvents were purchased from commercial suppliers e.g. Acros, Sigma-Aldrich, Fluorochem, Key Organics and Merck. All solvents were either analytical reagent or HPLC grade and were supplied by Fisher Scientific. Dry solvents were used for all reactions and were purchased from Sigma-Aldrich and VWR. The petroleum ether had a boiling point of 40 to 60 °C. CDCl₃ was supplied by Cambridge Isotope Laboratories, Inc., MeOD₄ was supplied by Sigma-Aldrich. All reactions were monitored for completion using TLC. Therefore, commercially available precoated silica gel 60 F₂₅₄ aluminum plates from Merck were used. Visualization of the spots was carried using the UV-lamp ($\lambda = 254$ nm) and stained with KMnO₄ or iodine and subsequently heated. Flash column chromatography was carried out using silica gel, technical grade, pore size 60 Å, 230–400 mesh particle size, 40–60 μ m particle size purchased from Sigma-Aldrich. The ¹³C- and ¹H NMR spectra were recorded using a Bruker AV (II) 500 spectrometer with a magnetic field strength of 9.4T. This is corresponding to a resonance frequency of 400 MHz for protons and around 100 MHz for the ¹³C nucleus. All ¹³C NMR are ¹H-broadband-decoupled. The chemical shifts δ are given in [ppm] and all coupling constants J are given in [Hz]. The spectra are referenced to the signal of the deuterated solvent: CDCl₃ ($\delta_{\text{H}} = 7.26$, $\delta_{\text{C}} = 77.16$ ppm) or MeOD₄ ($\delta_{\text{H}} = 3.31$, $\delta_{\text{C}} = 49.00$ ppm). The following abbreviations were used to describe signal shapes and multiplicity: s (singlet), bs (broad singlet), d (doublet), dd (doublet of doublet), ddd (doublet of doublet of a doublet), dddd (doublet of a doublet of a doublet of a doublet), t (triplet), dt (doublet of a triplet), q (quartet), dq (doublet of a quartet) and m (multiplet). Furthermore, 2D-NMR experiments: COSY and HSQC were used for the assignment of the signals and the processing of the NMR data was carried out using the NMR software TopSpin 3.0. All high-resolution mass spectra (HRMS)-time to flight electrospray were recorded on a Waters 2795 spectrometer by electrospray ionization (TOF ES) and the LC-MS spectra were performed on a Shimadzu UFLCXR system coupled to an Applied Biosystems API2000, and visualized at 220 nm (channel 2) and 254 nm (channel 1). LC-MS was carried out using a Phenomenex Gemini-NX C18 110A, column (50 mm \times 2 mm \times 3 μ m) at a flow rate 0.5 mL/min over a 5 min period - method (A). Analytical RP-HPLC was performed using a Waters 2767 sample manager, Waters 2525 binary gradient module, and visualized at 220 nm with a Waters 2487 dual wavelength absorbance detector - method (B). Spectra were analyzed using MassLynx. Preparative HPLC was performed using a Phenomenex Gemini-NX 5u C18 110A, AXIA packed column (160 mm \times 21.2 mm) at a flow rate of 20 mL/min, typically starting with 90% water/10% acetonitrile and progressing to 100% acetonitrile over 40 min. The water phase contained 0.01% ammonia. Chiral analytical HPLC was performed using a Phenomenex LC Lux 5u Amylose-2 packed column (250 \times 4.6 mm) at a flow rate of 1.5 mL/min, isocratically using 70% hexane: 30% ethanol supplemented with 0.2% DEA over 30 min - method (C).

All compounds submitted for biological screening had a purity >95% determined through either methods (A), (B) or (C).

General Procedure 1,2,4-Triazole Formation. To a solution of ethyl 2-thioxooctahydro-1, 6-naphthyridine-6(2H)-carboxylate (**15** and **16**) (2.43 mmol, 1 equiv) in toluene (20 mL) was added the corresponding hydrazide (4.86 mmol, 2 equiv) and the mixture was refluxed at 110 °C for 48 h. The solvent was evaporated and the crude product was purified by flash chromatography (dichloromethane/methanol 10:1) to yield the substituted triazoles (**17**–**23**).

General Procedure for the Removal of the Carbamate Protecting Group. To a solution of the protected substituted triazole (**17**–**23**, 0.41 mmol, 1 equiv) in ethanol (0.44 mL) and water (2.50 mL) was added KOH (1.80 mmol, 2.0–4.4 equiv) and the mixture was refluxed at 110 °C for 20 h. The reaction mixture was extracted with DCM (10 mL). The organic phase was dried over MgSO₄, filtered and the solvent was evaporated and the crude product was used without further purification.

(R)-3-Amino-1-((5S,9R)-1-(trifluoromethyl)-4,5,5a,8,9,9a-hexahydro-1,2,4-triazolo[4,3-a][1,6]naphthyridin-7(6H)-yl)-4-(2,4,5-trifluorophenyl)butan-1-one Hydrochloride (2). By the general experimental procedures outlined above (R)-3-amino-1-((5S,9R)-1-(trifluoromethyl)-4,5,5a,8,9,9a-hexahydro-1,2,4-triazolo[4,3-a][1,6]naphthyridin-7(6H)-yl)-4-(2,4,5-trifluorophenyl)butan-1-one hydrochloride was prepared from ethyl (4S, 8R)-2-thioxooctahydro-1,6-naphthyridine-6(2H)-carboxylate **12**.

¹H NMR (400 MHz, MeOD₄) δ 7.46–7.36 (m, 1H), 7.27–7.18 (m, 1H), 4.68 (t, $J = 17.5$ Hz, 1H), 4.01 (dd, $J = 15.7$, 30.6 Hz, 1H), 3.86 (bs, 1H), 3.76–3.50 (m, 1H), 3.39–3.25 (m, 2H), 3.22–3.07 (m, 3H), 2.92–2.81 (m, 3H), 2.49 (m, 1H), 2.18–2.10 (m, 2H), 2.02–1.94 (m, 2H) ppm. LC/MS m/z : 462.2 [M + H]⁺, 2.02 min. HPLC: > 98% (method A), 93:7 mixture of enantiomers (method C).

Ethyl (3R,4S)-3-(3-Ethoxy-3-oxopropyl)-4-(((R)-1-(4-methoxyphenyl)ethyl)amino)piperidine-1-carboxylate (10). To ethyl 3-(3-ethoxy-3-oxopropyl)-4-oxopiperidine-1-carboxylate (2.0 g, 7.4 mmol, 1 equiv) in 1,2 dichloroethane (32 mL) was added (S)-1-(4-methoxy-phenyl) ethylamine (1.2 mL, 7.9 mmol, 1.1 equiv) and NaBH(OAc)₃ (2.2 g, 10.4 mmol, 1.4 equiv) and the reaction was stirred overnight. The reaction mixture was diluted with saturated aqueous NaHCO₃ (50 mL) and the aqueous phase was extracted with ethyl acetate (3 \times 50 mL). The combined organic phases were dried over Na₂SO₄, filtered and the solvent was evaporated under reduced pressure. The crude product was purified using flash chromatography (ethyl acetate/petrol ether + NH₄OH, 10:1) to yield amine **10** (600 mg, 20%).

¹H NMR (400 MHz, CDCl₃) δ /ppm 7.19 (d, $J = 9.2$ Hz, 2H), 6.84 (d, $J = 8.1$ Hz, 2H), 4.18–4.04 (m, 6H), 3.78 (s, 5H), 2.83–2.74 (m, 2H), 2.61–2.57 (m, 1H), 2.51–2.28 (m, 1H), 1.83–1.68 (m, 2H), 1.48–1.37 (m, 4H), 1.30–1.20 (m, 9H) ppm. ¹³C NMR (100 MHz, CDCl₃) δ /ppm 173.8, 158.6, 155.9, 137.9, 127.6, 113.9, 61.3, 60.4, 55.4, 54.0, 44.9, 40.8, 36.6, 32.2, 25.1, 19.1, 14.7 ppm. LC/MS m/z : 407.6 [M + H]⁺.

Ethyl (4S,8R)-2-Oxooctahydro-1,6-naphthyridine-6(2H)-carboxylate (11). To (3R, 4S)-3-(3-ethoxy-3-oxopropyl)-4-(((R)-1-(4-methoxyphenyl) ethyl) amino) piperidine-1-carboxylate **10** (600 mg, 1.5 mmol, 1 equiv) in ethanol was added ammonium formate (400 mg, 6.3 mmol, 4.2 equiv) and Pd/C (small spatula) and heated to 50 °C for 8 h. The reaction mixture was filtered over Celite and the filtrate was evaporated under reduced pressure. The crude product was purified by flash chromatography (ethyl acetate/petrol ether 10:1 + 10% methanol) to yield lactam **11** (150 mg, 51%) as colorless oil.

¹H NMR (400 MHz, CDCl₃) δ 7.33 (bs, 1H), 4.11–4.04 (m, 2H), 3.57–3.51 (m, 3H), 3.40–3.36 (m, 1H), 3.26–3.20 (m, 1H), 3.15 (t, $J = 6.9$ Hz, 2H), 2.03–1.98 (m, 1H), 1.86–1.62 (m, 4H), 1.20 (t, $J = 7.2$ Hz, 3H) ppm. ¹³C NMR (100 MHz, CDCl₃) δ 172.6, 155.6, 61.7, 50.6, 44.7, 40.5, 32.7, 30.5, 28.9, 22.0, 14.9 ppm. HRMS m/z : C₁₄H₁₉N₂O₃ calculated 227.1390 [M + H]⁺, found 227.6533.

Ethyl (4S,8R)-2-Thioxooctahydro-1,6-naphthyridine-6(2H)-carboxylate (12). To a solution of ethyl (4R, 8S)-2-oxooctahydro-1,6-naphthyridine-6(2H)-carboxylate **10** (80 mg, 0.35 mmol, 1.0 equiv) in toluene (1 mL) was added Lawesson's reagent (71 mg, 0.17 mmol, 0.5 equiv) and the mixture was refluxed for 20 min. The reaction mixture was evaporated under reduced pressure and purified by flash chromatography (ethyl acetate/petrol ether: 10:1) to yield ethyl (4S, 8R)-2-thioxooctahydro-1, 6-naphthyridine-6(2H)-carboxylate **12** as a colorless waxy oil (90%). ¹H NMR (400 MHz, CDCl₃) δ 9.83 (bs, 1H), 4.11–4.04 (m, 2H), 3.60–3.50 (m, 3H), 3.40–3.34 (m, 1H), 3.26–3.17 (m, 1H), 2.94–2.77 (m, 2H), 2.05–2.01 (m, 1H), 1.81–1.70 (m, 4H), 1.19 (t, $J = 7.0$ Hz, 3H) ppm. ¹³C NMR (100 MHz, CDCl₃) δ 202.1, 155.7, 61.7, 53.1, 44.9, 40.6, 37.7, 31.7, 29.3, 21.4,

14.9 ppm. HRMS m/z : $C_{11}H_{19}H_2O_2S$ calculated 243.1162 $[M + H]^+$, found 243.0112.

rel-Ethyl (5S,9R)-1-Methyl-4,5,5a,8,9,9a-hexahydro-[1,2,4]-triazolo[4,3-a][1,6]naphthyridine-7(6H)-carboxylate (17). 1H NMR (400 MHz, $CDCl_3$) δ 4.20 (bs, 2H), 4.11–4.00 (m, 3H), 3.08–2.96 (m, 2H), 2.78–2.67 (m, 2H), 2.31 (s, 3H), 2.12–2.08 (m, 1H), 1.95–1.75 (m, 3H), 1.60 (qd, $J = 5.6$, 13.3 Hz, 1H), 1.16 (t, $J = 7.1$ Hz, 3H) ppm. ^{13}C NMR (100 MHz, $CDCl_3$) δ 155.5, 149.8, 148.9, 61.6, 51.8, 47.2, 42.1, 33.7, 28.1, 20.9, 19.3, 14.5, 10.3 ppm. HRMS m/z : $C_{13}H_{21}N_4O_2$ calc. 265.1659 $[M + H]^+$, found 265.2795.

rel-Ethyl (5S,9R)-1-Isopropyl-4,5,5a,8,9,9a-hexahydro-[1,2,4]-triazolo[4,3-a][1,6]naphthyridine-7(6H)-carboxylate (18, 75% yield). 1H NMR (400 MHz, $CDCl_3$) δ 4.26 (bs, 2H), 4.18–4.07 (m, 2H), 3.13 (dd, $J = 5.6$, $J = 17.0$ Hz, 1H), 3.08 (bs, 1H), 2.91–2.77 (m, 4H), 2.16 (d, $J = 11.1$ Hz, 1H), 2.03–1.92 (m, 1H), 1.90–1.84 (m, 2H), 1.70 (ddd, $J = 3.9$, 12.5, 26.1 Hz, 1H), 1.40 (d, $J = 6.6$ Hz, 3H), 1.30 (d, $J = 6.9$ Hz, 3H), 1.22 (t, $J = 7.3$ Hz, 3H) ppm. ^{13}C NMR (100 MHz, $CDCl_3$) δ 174.1, 157.7, 155.7, 149.4, 61.8, 52.2, 42.8, 33.9, 29.1, 22.7, 21.3, 21.1, 19.7, 14.6 ppm. HRMS m/z : $C_{15}H_{25}N_4O_2$ calc. 293.1972 $[M + H]^+$, found 293.1961.

rel-Ethyl (5S,9R)-1-Benzyl-4,5,5a,8,9,9a-hexahydro-[1,2,4]-triazolo[4,3-a][1,6]naphthyridine-7(6H)-carboxylate (19, 54% yield). 1H NMR (400 MHz, $MeOD_4$) δ 7.32–7.17 (m, 5H), 4.25–4.03 (m, 7H), 3.11–3.03 (dd, $J = 6.0$, 17.0, 2H), 2.87–2.75 (ddd, $J = 7.7$, 12.1, 19.8 Hz, 2H), 2.09 (d, $J = 10.9$ Hz, 1H), 1.89–1.83 (m, 1H), 1.79 (dq, $J = 4.8$, 12.1 Hz, 1H), 1.67–1.56 (m, 2H), 1.22 (t, $J = 7.4$ Hz, 3H) ppm. ^{13}C NMR (100 MHz, $MeOD_4$) δ 173.0, 157.3, 153.3, 136.5, 129.9, 129.4, 127.8, 62.7, 53.4, 43.1, 41.4, 34.7, 31.2, 28.9, 21.5, 19.9, 14.8 ppm. LCMS m/z : 341.4 $[M + H]^+$.

rel-Ethyl (5S,9R)-1-(Pyridin-2-yl)-4,5,5a,8,9,9a-hexahydro-[1,2,4]-triazolo[4,3-a][1,6]naphthyridine-7(6H)-carboxylate (20, 31% yield). 1H NMR (400 MHz, $CDCl_3$) δ 8.54 (d, 0.67H), 8.47 (m, 0.33H), 8.24 (d, $J = 8.0$ Hz, 0.67H), 8.0 (d, $J = 9.0$ Hz, 0.33H), 7.82–7.71 (m, 1H), 7.36 (t, $J = 6.5$ Hz, 0.33H), 7.26 (t, $J = 5.2$ Hz, 0.67H), 5.43 (dt, $J = 2.9$, 10.4 Hz, 1H), 4.22 (bs, 2H), 4.11–4.04 (m, 2H), 3.28 (bd, $J = 15.0$ Hz, 1H), 3.12 (bs, 1H), 2.94–2.78 (m, 2H), 2.32 (d, $J = 15.0$ Hz, 1H), 2.08–1.96 (m, H-3, 2H), 1.87 (bs, 1H), 1.55 (ddd, $J = 4.6$, 12.8, 24.5 Hz, 1H), 1.19 (t, $J = 6.8$ Hz, 3H) ppm. ^{13}C NMR (100 MHz, $CDCl_3$) δ 155.8, 148.8, 148.5, 148.4, 126.9, 126.7 (2), 125.5, 122.8, 122.6, 122.2, 61.7, 54.4, 50.5, 47.4, 42.6, 40.4, 21.4, 19.2, 14.7 ppm. LCMS m/z : 328.2 $[M + H]^+$.

rel-Ethyl (5S,9R)-1-(Pyrazin-2-yl)-4,5,5a,8,9,9a-Hexahydro-[1,2,4]-triazolo[4,3-a][1,6]naphthyridine-7(6H)-carboxylate (21, 33% yield). 1H NMR (400 MHz, $CDCl_3$) δ 9.56 (s, 0.7 H), (s, 0.3 H), 8.56, 8.54, 8.53, 8.50, 8.49 (ms, 2H), 5.28 (dt, $J = 4.2$, 11.3 Hz, 1H), 4.26 (bs, 2H), 4.15–4.07 (m, 2H), 3.29 (dd, $J = 6.1$, 17.5 Hz, 1H), 3.13 (bs, 1H), 2.96 (ddd, $J = 8.1$, 12.3, 19.7 Hz, 1H), 2.84 (m, 1H), 2.27 (d, $J = 13.5$ Hz, 1H), 2.09–2.02 (m, 2H), 1.93 (bs, 1H), 1.63 (dq, $J = 4.5$, 12.2 Hz, 1H), 1.22 (t, $J = 6.7$ Hz, 3H) ppm. ^{13}C NMR (100 MHz, $CDCl_3$) δ 163.3, 155.7, 152.6, 148.3, 147.7, 144.8, 144.2, 144.1, 143.8, 142.9, 142.8, 61.7, 54.5, 47.4, 42.6, 34.0, 28.9, 21.5, 19.3, 14.7 ppm. LCMS m/z : 329.1 $[M + H]^+$.

rel-Ethyl (5S,9R)-1-(2-Methylthiazol-4-yl)-4,5,5a,8,9,9a-hexahydro-[1,2,4]-triazolo[4,3-a][1,6]naphthyridine-7(6H)-carboxylate (22, 75% yield). 1H NMR (400 MHz, $CDCl_3$) δ 8.11 (s, 1H), 5.22 (dt, $J = 4.2$, 11.9 Hz, 1H), 4.26 (bs, H-4, 2H), 4.17–4.09 (m, 2H), 3.24 (dd, $J = 5.1$, 16.7 Hz, 1H), 3.15 (bs, 1H), 2.92 (ddd, $J = 7.2$, 12.4, 20.1 Hz, 1H), 2.80 (bs, 1H), 2.75 (s, 3H), 2.25 (d, $J = 11.2$ Hz, 1H), 2.09–2.05 (m, 2H), 1.92 (bs, 1H), 1.60 (dq, $J = 5.4$, 12.5 Hz, 1H), 1.24 (t, $J = 7.1$ Hz, 3H) ppm. ^{13}C NMR (100 MHz, $CDCl_3$) δ 166.7, 155.9, 150.8, 147.5, 142.6, 120.2, 61.8, 54.1, 47.5, 42.7, 34.0, 28.9, 21.5, 19.7, 19.5, 14.8 ppm. LCMS m/z : 348.2 $[M + H]^+$.

rel-Ethyl (5R,9R)-1-Isopropyl-4,5,5a,8,9,9a-hexahydro-[1,2,4]-triazolo[4,3-a][1,6]naphthyridine-7(6H)-carboxylate (23, 30% yield). 1H NMR (400 MHz, $CDCl_3$) δ 4.31 (m, 2H), 4.09 (q, $J = 6.8$ Hz, 2H), 3.66 (dt, $J = 3.8$, 11.1 Hz, 1H), 3.14 (ddd, $J = 1.5$, 4.1, 16.0 Hz, 1H), 3.03 (sept, $J = 6.7$ Hz, 1H), 2.91 (bs, 1H), 2.79 (ddd, $J = 6.0$, 13.1, 19.5 Hz, 1H), 2.66 (bs, 1H), 2.59 (bs, 1H), 1.87 (dd, $J = 6.1$, 13.3 Hz, 1H), 1.78–1.62 (m, 2H), 1.49 (ddd, $J = 4.6$, 12.7, 25.0 Hz, 2H), 1.38 (d, $J = 6.6$ Hz, 3H), 1.28 (d, $J = 7.1$ Hz, 3H), 1.21 (t, $J = 6.1$ Hz, 3H) ppm. ^{13}C NMR (100 MHz, $CDCl_3$) δ 174.1, 158.3, 155.2, 151.1,

61.8, 59.6, 47.8, 42.5, 41.3, 33.4, 30.8, 24.2, 22.8, 21.5, 21.1 ppm. HRMS m/z : $C_{15}H_{23}N_4O_2$ calc. 293.1972 $[M + H]^+$, found 293.1517.

rel-(5S,9R)-1-Methyl-4,5,5a,6,7,8,9,9a-octahydro-[1,2,4]triazolo[4,3-a][1,6]naphthyridine (24, 65% Yield). 1H NMR (400 MHz, $CDCl_3$) δ 4.03 (dt, $J = 5.1$, 11.7 Hz, 1H), 3.17–3.07 (m, 3H), 2.98 (dd, $J = 4.1$, 12.7 Hz, 1H), 2.83–2.73 (qd, $J = 6.5$, 12.7 Hz, 1H), 2.67 (dt, $J = 3.1$, 13.1 Hz, 1H), 2.36 (s, 3H), 2.28 (ddd, $J = 7.6$, 13.8, 23.8 Hz, 1H), 2.06–2.01 (m, 1H), 1.94 (bs, 1H), 1.88–1.82 (m, 1H), 1.79–1.73 (m, 1H), 1.63 (ddd, $J = 4.8$, 12.6, 25.3 Hz, 1H) ppm. ^{13}C NMR (100 MHz, $CDCl_3$) δ 150.5, 149.2, 52.6, 50.6, 45.2, 34.1, 29.7, 21.6, 20.2, 10.5 ppm. HRMS m/z : $C_{10}H_{17}N_4$ calc. 193.1448 $[M + H]^+$, found 193.1507.

rel-(5S,9R)-1-Isopropyl-4,5,5a,6,7,8,9,9a-octahydro-[1,2,4]triazolo[4,3-a][1,6]naphthyridine (25, 68% Yield). 1H NMR (400 MHz, $CDCl_3$) δ 4.07 (dt, $J = 4.8$, 10.2 Hz, 1H), 3.18–3.07 (m, 3H), 3.00–2.97 (dd, $J = 3.7$, 12.8 Hz, 1H), 2.91–2.75 (m, 2H), 2.67 (dt, $J = 3.3$, 12.8 Hz, 1H), 2.36–2.23 (m, 1H), 2.04 (bd, $J = 13.7$ Hz, 1H), 1.85–1.82 (m, 1H), 1.78–1.71 (m, 2H), 1.67 (ddd, $J = 4.4$, 12.8, 24.9 Hz, 1H), 1.39 (d, $J = 6.7$ Hz, 3H), 1.30 (d, $J = 6.7$ Hz, 3H) ppm. HRMS m/z : $C_{12}H_{21}N_4$ calc. 221.1761 $[M + H]^+$, found 221.1447.

rel-(5S,9R)-1-Benzyl-4,5,5a,6,7,8,9,9a-octahydro-[1,2,4]triazolo[4,3-a][1,6]naphthyridine (26, 80% Yield). 1H NMR (400 MHz, $CDCl_3$) δ 7.30–7.20 (m, 5H), 4.25 (d, $J = 16.3$ Hz, 1H), 4.02 (d, $J = 16.3$ Hz, 1H), 3.83 (dt, $J = 5.3$, 11.4, 1H), 3.18 (ddd, $J = 1.7$, 6.5, 17.1 Hz, 1H), 3.09–3.00 (m, 2H), 2.53 (dt, $J = 3.4$, 12.3 Hz, 1H), 2.29 (ddd, $J = 5.9$, 12.9, 26.0 Hz, 1H), 1.94 (m, 1H), 1.77–1.56 (m, 2H) ppm. HRMS m/z : $C_{16}H_{21}N_4$ calc. 269.1761 $[M + H]^+$, found 269.2529.

rel-(5S,9R)-1-(6-Ethoxypyridin-2-yl)-4,5,5a,6,7,8,9,9a-octahydro-[1,2,4]triazolo[4,3-a][1,6]naphthyridine (27, 67% Yield). 1H NMR (400 MHz, $CDCl_3$) δ 7.90 (dd, $J = 0.8$, 7.6 Hz, 1H), 7.66 (dd, $J = 6.8$, 8.2 Hz, 1H), 6.74 (dd, $J = 0.8$, 8.2 Hz, 1H), 5.36 (dt, $J = 5.0$, 11.7 Hz, 1H), 4.42–4.24 (m, 2H), 3.31 (ddd, $J = 1.0$, 5.6, 17.4 Hz, 1H), 3.23 (t, $J = 13.1$ Hz, 1H), 3.13 (m, 1H), 3.04 (dd, $J = 3.3$, 12.4 Hz, 1H), 2.95 (ddd, $J = 6.0$, 12.5, 17.2 Hz, 1H), 2.66 (td, $J = 3.0$, 13.0 Hz, 3H), 2.41 (ddd, $J = 5.6$, 13.0, 25.9 Hz, 1H), 2.27–2.22 (m, 1H), 2.14–2.09 (m, 1H), 1.88–1.81 (m, 1H), 1.68 (ddd, $J = 4.1$, 12.5, 24.5 Hz, 1H), 1.42 (t, $J = 7.1$ Hz, 3H) ppm. HRMS m/z : $C_{16}H_{22}N_5O$ calc. 300.1819 $[M + H]^+$, found 300.4049.

rel-(5S,9R)-1-(Pyridin-2-yl)-4,5,5a,6,7,8,9,9a-octahydro-[1,2,4]triazolo[4,3-a][1,6]naphthyridine (28, 59% Yield). 1H NMR (400 MHz, $CDCl_3$) δ 8.57 (dq, $J = 0.8$, 4.4 Hz, 1H), 8.25 (dt, $J = 1.0$, 8.1 Hz, 1H), 7.75 (dt, $J = 1.9$, 7.9 Hz, 1H), 7.26 (dd, $J = 1.2$, 4.2 Hz, 1H), 5.38 (dt, $J = 5.3$, 12.2 Hz, 1H), 3.28 (ddd, $J = 1.3$, 5.9, 17.0 Hz, 1H), 3.13 (m, 1H), 3.06–2.99 (m, 2H), 2.91 (ddd, $J = 6.8$, 12.1, 17.6 Hz, 1H), 2.68 (dt, $J = 2.8$, 12.7 Hz, 1H), 2.35 (ddd, $J = 5.8$, 13.1, 26.2 Hz, 1H), 2.21–2.15 (m, 1H), 2.10–1.94 (m, 2H), 1.83–1.76 (m, 1H), 1.53 (ddd, $J = 4.3$, 12.5, 25.5 Hz, 1H) ppm. LCMS m/z : 256.0 $[M + H]^+$, 0.42 min.

rel-(5S,9R)-1-(Pyrazin-2-yl)-4,5,5a,6,7,8,9,9a-octahydro-[1,2,4]triazolo[4,3-a][1,6]naphthyridine (29, 54% Yield). 1H NMR (400 MHz, $CDCl_3$) δ 9.55 (d, $J = 1.3$ Hz, 1H), 8.56–8.55 (m, 2H), 5.24 (dt, $J = 4.8$, 11.0 Hz, 1H), 3.33 (ddd, $J = 1.0$, 5.8, 17.0 Hz, 1H), 3.17 (dt, $J = 1.6$, 13.0 Hz, 1H), 3.10–3.03 (m, 2H), 2.96 (ddd, $J = 7.0$, 12.6, 17.3 Hz, 1H), 2.71 (dt, $J = 2.6$, 12.6 Hz, 1H), 2.40 (ddd, $J = 5.8$, 12.6, 25.8 Hz, 1H), 2.19–2.03 (m, 1H), 1.90–1.80 (m, 4H), 1.60 (ddd, $J = 4.7$, 12.4, 24.2 Hz, 1H) ppm.

rel-2-Methyl-4-((5S,9R)-4,5,5a,6,7,8,9,9a-octahydro-[1,2,4]triazolo[4,3-a][1,6]naphthyridin-1-yl)thiazole (30, 87% Yield). 1H NMR (400 MHz, $CDCl_3$) δ 7.91 (s, 1H), 5.16–5.10 (m, 1H), 3.26 (dd, $J = 6.1$, 16.9 Hz, 1H), 3.14 (m, 1H), 3.07–3.02 (m, 2H), 2.94–2.84 (m, 1H), 2.73 (s, 3H), 2.69–2.62 (t, $J = 11.2$ Hz, 1H), 2.36 (ddd, $J = 5.1$, 12.7, 25.9 Hz, 1H), 2.16 (d, $J = 14.1$ Hz, 1H), 1.94 (d, $J = 12.5$ Hz, 1H), 1.83–1.77 (m, 2H), 1.60–1.50 (m, 1H) ppm. LC/MS m/z : 276.2 $[M + H]^+$.

rel-(5R,9R)-1-Isopropyl-4,5,5a,6,7,8,9,9a-octahydro-[1,2,4]triazolo[4,3-a][1,6]naphthyridine (31, 48% Yield). 1H NMR (400 MHz, $CDCl_3$) δ 3.64 (dt, $J = 3.3$, 11.2 Hz, 1H), 3.25–3.17 (m, 1H), 3.17–3.04 (m, 3H), 2.86–2.78 (m, 2H), 2.61–2.54 (m, 2H), 2.03 (bs, 1H), 1.83–1.64 (m, 3H), 1.54–1.46 (ddd, $J = 4.3$, 11.1, 23.2 Hz, 1H),

1.42 (d, J = 6.7 Hz, 3H), 1.30 (d, J = 6.7 Hz, 3H) ppm. HRMS m/z : $C_{12}H_{21}N_4$ calc. 221.1761 [M + H]⁺, found 221.1684.

General Procedure for Amide Coupling. To a solution of amine (**24-31**, 0.33 mmol, 1 equiv) in DMF (1 mL) was added (*R*)-3-((*tert*-butoxycarbonylamino)-4-(2,4,5-trifluorophenyl)butanoic acid EDCl (0.38 mmol, 1.2 equiv) and HOBT (0.38 mmol, 1.2 equiv) and the mixture was stirred at RT overnight. The reaction mixture was diluted with ethyl acetate (20 mL) and saturated aqueous NaHCO₃ (20 mL). The water phase was extracted with ethyl acetate (3 × 20 mL). The combined organic phases were washed with saturated aqueous sodium chloride (20 mL), dried over Na₂SO₄, filtered and the crude product was purified by flash chromatography (dichloromethane/methanol: 10:1) to yield the amide.

General Method for Boc-Deprotection. To the above amides (**32-39**, 0.08 mmol, 1 equiv) was added 4 N HCl in 1,4-dioxane (0.5 mL) and the reaction mixture was stirred at RT for 30 min. The excess hydrogen chloride solution was evaporated under N₂ gas to yield the hydrochloride salt of the amines as oils.

rel-tert-Butyl ((R)-4-((5S,9R)-1-Methyl-4,5,5a,8,9,9a-hexahydro[1,2,4]triazolo[4,3-a][1,6]naphthyridin-7(6H)-yl)-4-oxo-1-(2,4,5-trifluorophenyl)butan-2-yl)carbamate (32, 45% Yield). ¹H NMR (400 MHz, MeOD₄) δ 7.22–7.16 (m, 1H), 7.14–7.04 (m, 1H), 6.68–6.56 (m, 1H), 4.72 (t, J = 13.8 Hz, 0.5H), 4.63 (m, 0.5H), 4.54–4.46 (m, 1H), 4.23–4.01 (m, 2H), 3.56–3.48 (m, 0.5H), 3.35–3.24 (m, 3H), 3.14–2.47 (m, 6H), 2.44 (s, Me, 3H), 2.35–2.27 (m, 1H), 2.14–1.63 (m, 3H), 1.34–1.24 (3s, 9H) ppm. HRMS m/z : $C_{25}H_{33}N_3F_3O_3$ calc. 508.2530 [M + H]⁺, found 508.3067.

tert-Butyl ((R)-4-((5S,9R*)-1-Isopropyl-4,5,5a,8,9,9a-hexahydro[1,2,4]triazolo[4,3-a][1,6]naphthyridin-7(6H)-yl)-4-oxo-1-(2,4,5-trifluorophenyl)butan-2-yl)carbamate (33; 64% Yield).* ¹H NMR (400 MHz, CDCl₃) δ 7.07–7.00, 6.89 (m, 1H), 5.56–5.37 (m, 1H), 4.82–4.72 (m, 1H), 4.24–4.20 (m, 1H), 4.10 (bs, 1H), 4.00–3.89 (m, 1H), 3.38 (m, 0.5H), 3.17–3.08 (m, 1.5H), 2.97–2.80 (m, 4H), 2.71–2.47 (m, 3H), 2.23 (bs, 1H), 1.99–1.62 (m, 4H), 1.42–1.39 (m, 3H), 1.32–1.30 (m, 12H) ppm. ¹³C NMR (100 MHz, CDCl₃) δ 169.7, 157.7, 157.4, 155.0, 149.4, 149.1, 147.9, 147.7, 145.4, 143.2, 128.6, 126.5, 124.4, 121.8, 119.2, 112.1, 110.3, 105.1, 79.6, 52.1, 49.2, 48.4, 45.1, 44.2, 44.1, 40.1, 34.0, 33.9, 33.8, 28.9, 26.4, 24.5, 21.7, 21.2, 19.6, 19.4 ppm. HRMS m/z : $C_{27}H_{37}N_3F_3O_3$ calc. 536.2843 [M + H]⁺, found 536.2856.

(R)-3-Amino-1-((5S,9R*)-1-benzyl-4,5,5a,8,9,9a-hexahydro[1,2,4]triazolo[4,3-a][1,6]naphthyridin-7(6H)-yl)-4-(2,4,5-trifluorophenyl)butan-1-one Hydrochloride (34, 98% Yield).* HPLC (t_R = 11.01 min, 100%). ¹H NMR (400 MHz, MeOD₄) δ 7.41–7.29 (m, 5H), 7.26–7.20 (m, 2H), 4.75–4.64 (m, 1H), 4.39 (q, 2H), 3.89–3.76 (m, 3H), 3.13–2.99 (m, 4H), 2.79–2.55 (m, 4H), 2.09–1.67 (m, 3H) ppm. ¹³C NMR (100 MHz, MeOD₄) δ 173.1, 170.4, 169.9, 159.0, 157.0, 152.1, 151.9, 150.1, 149.9, 149.3, 149.1, 147.3, 130.2, 130.1, 128.9, 120.4, 107.0, 54.6, 45.7, 44.7, 36.4, 36.3, 34.8, 34.2, 32.4, 32.3, 30.9, 30.7, 29.0, 28.4, 20.8, 18.7 ppm. HRMS m/z : $C_{26}H_{29}N_3F_3O$ calc. 484.2389 [M + H]⁺, found 484.2330.

tert-Butyl ((R)-4-((5S,9R*)-1-(6-Ethoxy-pyridin-2-yl)-4,5,5a,8,9,9a-hexahydro[1,2,4]triazolo[4,3-a][1,6]naphthyridin-7(6H)-yl)-4-oxo-1-(2,4,5-trifluorophenyl)butan-2-yl)carbamate (35, 98% Yield).* ¹H NMR (400 MHz, CDCl₃) δ 8.07–7.95 (m, 1H), 7.82–7.72 (m, 1H), 7.61–7.51 (m, 0.5H), 7.50–7.40 (m, 0.5H), 7.13–7.02 (m, 1H), 6.98–6.86 (m, 1H), 5.70–5.34 (m, 1H), 5.00–4.75 (m, 1H), 4.43–4.33 (m, 1H), 4.29–4.22 (m, 0.5H), 4.14–3.87 (m, 1.5H), 3.61–3.45 (m, 3H), 3.16–2.82 (m, 6H), 2.74–2.41 (m, 2H), 2.38–2.26 (m, 1H), 2.16–1.90 (m, 2H), 1.81–1.69 (m, 1H), 1.48–1.30 (m, 12H) ppm. LC/MS m/z : 615.3 [M + H]⁺.

tert-Butyl ((R)-4-Oxo-4-((5S,9R*)-1-(pyridin-2-yl)-4,5,5a,8,9,9a-hexahydro[1,2,4]triazolo[4,3-a][1,6]naphthyridin-7(6H)-yl)-1-(2,4,5-trifluorophenyl)butan-2-yl)carbamate (36, 37% Yield).* ¹H NMR (400 MHz, CDCl₃) δ 8.60–8.57 (m, 1H), 8.29 (d, J = 7.9 Hz, 1H), 7.79 (dt, J = 1.3, 7.8 Hz, 1H), 7.32–7.28 (m, 1H), 7.08–7.00 (m, 1H), 6.89–6.80 (m, 1H), 5.60–5.40 (m, 2H), 4.83 (d, J = 14.0 Hz, 0.5 H), 4.72–4.65 (m, 0.5H), 4.13–4.01 (m, 1H), 3.92 (t, J = 15.1, 0.5H), 3.83–3.76 (m, 0.5H), 3.47–3.41 (m, 0.5H), 3.34–3.23 (m, 1H), 3.15 (dt, J = 2.7, 13.0 Hz, 0.5H), 3.03–2.85 (m, 4H), 2.70–2.47 (m, 3H), 2.40–2.32 (m, 1H), 2.27–2.15 (m, 1H), 2.10–1.91 (m, 1H), 1.66–

1.48 (m, 1H), 1.35–1.33 (m, 9H) ppm. ¹³C NMR (100 MHz, CDCl₃) δ 169.6, 169.4, 157.6, 155.4, 155.0, 151.9, 151.6, 150.4, 150.1, 148.8, 148.1, 147.8, 147.7, 145.4, 137.2, 124.0, 123.3, 119.3, 105.4, 79.5, 54.2, 49.3, 49.1, 48.5, 44.5, 40.5, 34.3, 34.2, 34.1, 34.0, 33.4, 33.1, 29.4, 28.3, 21.6, 21.5, 19.6, 19.4 ppm. LC/MS m/z : 571.2 [M + H]⁺.

tert-Butyl ((R)-4-Oxo-4-((5S,9R*)-1-(pyrazin-2-yl)-4,5,5a,8,9,9a-hexahydro[1,2,4]triazolo[4,3-a][1,6]naphthyridin-7(6H)-yl)-1-(2,4,5-trifluorophenyl)butan-2-yl)carbamate (37, 44% Yield).* ¹H NMR (400 MHz, CDCl₃) δ 8.68 (m, 1H, 1H), 7.80 (dd, J = 9.4 Hz, 1H), 7.43 (m, 1H), 7.09–7.01 (m, 1H), 6.90–6.86 (m, 1H), 5.51 (m, 1H), 4.86 (d, J = 12.5 Hz, 0.5H), 4.75 (m, 0.5H), 4.15–3.35 (m, 6H), 3.19–3.10 (m, 1H), 2.97–2.80 (m, 5H), 2.70–2.48 (m, 3H), 2.14–1.89 (m, 2H), 1.35–1.31 (m, 9H) ppm. ¹³C NMR (100 MHz, CDCl₃) δ 173.6, 159.9, 157.3, 155.3, 145.8, 145.3, 145.2, 143.3, 142.8, 128.7, 127.0, 126.8, 119.2, 117.0, 111.6, 105.7, 105.4, 105.3, 79.8, 55.9, 55.1, 49.1, 48.9, 47.7, 45.0, 44.3, 37.8, 36.6, 35.5, 33.6, 33.2, 29.4, 28.4, 25.4, 21.2 (2), 18.8, 18.6 ppm. HRMS m/z : $C_{28}H_{33}N_7F_3O_3$ calc. 572.2591 [M + H]⁺, found 572.2415.

tert-Butyl ((R)-4-((5S,9R*)-1-(2-Methylthiazol-4-yl)-4,5,5a,8,9,9a-hexahydro[1,2,4]triazolo[4,3-a][1,6]naphthyridin-7(6H)-yl)-4-oxo-1-(2,4,5-trifluorophenyl)butan-2-yl)carbamate (38, 69% Yield).* ¹H NMR (400 MHz, CDCl₃) δ 8.01 (s, 0.5H), 7.97 (s, 0.5H), 7.07–6.99 (m, 1H), 6.90–6.81 (m, 1H), 5.62–5.40 (m, 1H), 5.33–5.24 (m, 1H), 4.81–4.64 (m, 0.5H), 4.14 (bm, 1H), 3.98–3.77 (m, 0.5H), 3.46–3.04 (3t, 1H), 2.98–2.82 (m, 6H), 2.74 (s, 3H), 2.67–2.45 (m, 2H), 2.33 (m, 1H), 2.21–2.09 (m, 1H), 2.06–1.74 (m, 1H), 1.67–1.49 (m, 1H), 1.34–1.30 (2s, 9H) ppm. HRMS m/z : $C_{28}H_{34}N_6F_3O_3S$ calc. 591.2360 [M + H]⁺, found 591.2156.

tert-Butyl ((R)-4-((5R,9R*)-1-Isopropyl-4,5,5a,8,9,9a-hexahydro[1,2,4]triazolo[4,3-a][1,6]naphthyridin-7(6H)-yl)-4-oxo-1-(2,4,5-trifluorophenyl)butan-2-yl)carbamate (39, 77% Yield).* ¹H NMR (400 MHz, CDCl₃) δ 7.10–7.04 (m, 1H), 6.92–6.86 (m, 1H), 5.48–5.42 (m, 1H), 4.82 (dd, J = 13.2, 29.9 Hz, 1H), 4.14–3.93 (m, 1H), 3.79 (dt, J = 3.0, 10.9 Hz, 1H), 3.27–3.16 (m, 1H), 3.12–2.46 (m, 9H), 2.00–1.87 (m, 1H), 1.84–1.67 (m, 2H), 1.64–1.51 (m, 1H), 1.45, 1.43 (2s, 3H), 1.35 (s, 9H), 1.33, 1.32 (2s, 3H) ppm. ¹³C NMR (100 MHz, CDCl₃) δ 169.2, 158.5, 158.4, 157.5, 155.4, 155.0, 151.7, 151.5, 150.1, 147.8, 147.5, 145.5, 143.3, 128.7, 126.5, 124.4, 122.0, 121.8, 119.3, 119.0, 105.6, 105.4, 105.1, 79.6, 59.7, 59.5, 49.5, 48.4, 45.5, 44.3, 41.8, 41.2, 41.1, 36.6, 33.2, 31.4, 28.4, 27.0, 24.3, 22.8, 21.5, 21.2 ppm. HRMS m/z : $C_{27}H_{37}N_3F_3O_3$ calc. 536.2843 [M + H]⁺, found 536.2926.

(R)-3-Amino-1-((5S,9R*)-1-methyl-4,5,5a,8,9,9a-hexahydro[1,2,4]triazolo[4,3-a][1,6]naphthyridin-7(6H)-yl)-4-(2,4,5-trifluorophenyl)butan-1-one Hydrochloride (40).* ¹H NMR (400 MHz, MeOD₄) δ 7.45–7.38 (m, 1H), 7.29–7.21 (m, 1H), 4.81–4.66 (m, 2H), 4.08–4.02 (m, 0.5H), 3.99–3.94 (m, 0.5H), 3.89–3.82 (m, 1H), 3.57–3.49 (m, 0.5H), 3.31–3.18 (m, 1.5H), 3.15–3.03 (m, 3H), 2.94–2.73 (m, 2H), 2.64 (s, 3H), 2.44–2.40 (m, 1H), 2.20–1.87 (m, 4H) ppm. ¹³C NMR (100 MHz, MeOD₄) δ 170.3, 170.0, 153.0, 152.6, 120.7, 107.2, 107.0, 106.8, 54.4, 49.8, 45.7, 44.6, 41.0, 34.9, 34.8, 34.2, 34.0, 32.4, 28.8, 28.0, 24.2, 20.9, 19.0, 18.9, 9.8 ppm. LCMS m/z : 408.2, [M + H]⁺. HPLC (t_R = 9.60 min, 100% - method (b)).

(R)-3-Amino-1-((5S,9R*)-1-isopropyl-4,5,5a,8,9,9a-hexahydro[1,2,4]triazolo[4,3-a][1,6]naphthyridin-7(6H)-yl)-4-(2,4,5-trifluorophenyl)butan-1-one (41, 100% Yield).* ¹H NMR (400 MHz, MeOD₄) δ 7.40–7.32 (m, 1H), 7.30–7.21 (m, 1H), 4.69–4.62 (m, 3H), 4.02–3.96 (m, 0.5H), 3.93–3.80 (m, 2H), 3.55–3.48 (dt, J = 3.6, 11.6 Hz, 0.5H), 3.28–3.21 (m, 1H), 3.17–3.10 (m, 1H), 3.08–3.03 (m, 3H), 3.00–2.66 (m, 4H), 2.38 (d, J = 12.7 Hz, 1H), 2.09–1.74 (m, 4H), 1.42 (2d, J = 6.7 Hz, 6.7 Hz, 3H), 1.37 (2d, J = 6.7 Hz, 6.7 Hz, 3H) ppm. ¹³C NMR (100 MHz, MeOD₄) δ 170.4, 170.3, 170.0, 160.5, 152.7, 152.5, 128.8, 127.9, 120.7, 120.5, 118.3, 111.6, 107.2, 107.0, 106.8, 73.5, 72.4, 62.2, 54.7, 50.2, 45.6, 44.6, 41.0, 40.9, 34.9, 34.1, 33.9, 32.4, 29.6, 28.8, 21.9, 21.1, 20.7, 18.8 ppm. LC/MS m/z : 436.5 [M + H]⁺, 1.85 min. HPLC (t_R = 7.60 min, 100% - method (b)).

(R)-3-Amino-1-((5S,9R*)-1-(6-ethoxy-pyridin-2-yl)-4,5,5a,8,9,9a-hexahydro[1,2,4]triazolo[4,3-a][1,6]naphthyridin-7(6H)-yl)-4-(2,4,5-trifluorophenyl)butan-1-one Hydrochloride (43, 100% Yield).* ¹H NMR (400 MHz, MeOD₄) δ 7.80–7.75 (m, 1H), 7.47–7.38 (m, 1H), 7.36–7.29 (m, 1H), 7.27–7.20 (m, 1H), 6.89 (d, J = 8.1 Hz, 1H),

5.59–5.54 (m, 1H), 4.67–4.56 (m, 1H), 4.50–4.43 (m, 1H), 4.38–4.30 (m, 1H), 3.94–3.79 (m, 3H), 3.68–3.61 (m, 1H), 3.22–3.13 (m, 2H), 3.10–2.95 (m, 4H), 2.83–2.60 (m, 2H), 2.52–2.45 (m, 2H), 2.29–2.21 (m, 1H), 2.07–1.58 (m, 2H), 1.29 (s, 3H) ppm. HRMS *m/z*: C₂₆H₃₀N₆F₃O₂ calc. 515.2377 [M + H]⁺, found 515.2961. HPLC 98% - method (A).

(*R*)-3-Amino-1-((5*S**,9*R**)-1-(pyridin-2-yl)-4,5,5a,8,9,9a-hexahydro-[1,2,4]triazolo[4,3-*a*][1,6]naphthyridin-7(6*H*)-yl)-4-(2,4,5-trifluorophenyl)butan-1-one Hydrochloride (**44**, 100% Yield). ¹H NMR (400 MHz, MeOD₄) δ 8.81 (s, 1H), 8.26 (d, *J* = 7.4 Hz, 1H), 8.06 (t, *J* = 8.5 Hz, 1H), 7.64–7.61 (m, 1H), 7.46–7.39 (m, 1H), 7.29–7.19 (m, 1H), 5.81–5.73 (m, 1H), 4.76 (t, *J* = 11.9 Hz, 0.5H), 4.65 (d, *J* = 14.8 Hz, 0.5H), 4.32–4.21 (m, 0.5H), 4.17–4.06 (m, 1H), 3.96 (t, *J* = 12.9 Hz, 0.5H), 3.90–3.82 (m, 1H), 3.61–3.53 (m, 0.5H), 3.46–3.36 (m, 1H), 3.31–3.21 (m, 2H), 3.15–3.05 (m, 2H), 2.96–2.75 (m, 2H), 2.59–2.50 (m, 1H), 2.36 (t, *J* = 11.9 Hz, 1H), 2.24–2.09 (m, 1H), 2.07–1.96 (m, 1H), 1.92–1.80 (m, 1H) ppm. ¹³C NMR (100 MHz, MeOD₄) δ 170.4, 170.3, 170.0, 154.5, 151.5, 150.9, 146.1, 139.2, 127.4, 120.7, 107.2, 106.9, 57.2, 49.8, 45.8, 44.9, 41.3, 34.8, 34.3, 34.2, 32.4, 32.2, 29.4, 28.7, 21.4, 18.6, 18.5 ppm. HRMS *m/z*: C₂₄H₂₆N₆F₃O calc. 471.2115 [M + H]⁺, found 471.2754. HPLC (*t*_R = 10.75 min, 99% - method (B)).

(*R*)-3-Amino-1-((5*S**,9*R**)-1-(pyrazin-2-yl)-4,5,5a,8,9,9a-hexahydro-[1,2,4]triazolo[4,3-*a*][1,6]naphthyridin-7(6*H*)-yl)-4-(2,4,5-trifluorophenyl)butan-1-one Hydrochloride (**45**). ¹H NMR (400 MHz, MeOD₄) δ 9.42 (s, 1H), 8.81 (s, 1H), 8.78 (s, 1H), 7.44–7.31 (m, 1H), 7.29–7.20 (m, 1H), 5.59–5.55 (m, 1H), 4.76 (dd, *J* = 8.0, 13.6 Hz, 0.5H), 4.65 (dd, *J* = 12.5 Hz, 0.5H), 4.09–4.03 (m, 0.5H), 3.96–3.80 (m, 2H), 3.28–3.16 (m, 2H), 3.13–3.01 (m, 3H), 2.88–2.59 (m, 2H), 2.55–2.49 (m, 1H), 2.32 (t, *J* = 12.9 Hz, 1H), 2.19–2.05 (m, 1H), 2.03–1.92 (m, 1H), 1.86–1.76 (m, 1H) ppm. ¹³C NMR (100 MHz, MeOD₄) δ 173.1, 170.3, 170.2, 170.0, 147.0, 145.5, 145.3, 128.4, 20.6, 120.5, 107.2, 107.0, 56.9, 49.8, 45.8, 44.9, 41.3, 34.8, 34.7, 34.5, 32.4, 29.6, 28.9, 24.2, 21.3, 19.0 ppm. HRMS *m/z*: C₂₃H₂₄N₇F₃O calc. 472.2067 [M + H]⁺, found 472.2714. HPLC (*t*_R = 11.87 min, 99% - method (B)).

(*R*)-3-Amino-1-((5*S**,9*R**)-1-(2-methylthiazol-4-yl)-4,5,5a,8,9,9a-hexahydro[1,2,4]triazolo[4,3-*a*][1,6]naphthyridin-7(6*H*)-yl)-4-(2,4,5-trifluorophenyl)butan-1-one Hydrochloride (**46**, 68% Yield). ¹H NMR (400 MHz, MeOD₄) δ 8.23–8.22 (m, 1H), 7.42–7.34 (m, 1H), 7.30–7.20 (m, 1H), 5.49–5.43 (m, 1H), 4.75 (dd, *J* = 8.7, 14.1 Hz, 0.5H), 4.64 (d, *J* = 13.0 Hz, 0.5H), 4.06–4.00 (m, 0.5H), 3.95–3.52 (m, 1.5H), 3.59–3.52 (m, 1H), 3.29–3.19 (m, 0.5H), 3.17–3.05 (m, 3H), 2.96–2.83 (m, 2H), 2.81 (s, 3H), 2.80–2.69 (m, 2H), 2.49 (d, *J* = 13.5 Hz, 1H), 2.30–2.19 (m, 1H), 2.14–1.84 (m, 2H), 1.76 (ddd, *J* = 5.8, 12.8, 25.5 Hz, 1H) ppm. ¹³C NMR (100 MHz, MeOD₄) δ 170.3, 170.2, 169.9, 159.0, 157.0, 153.2, 153.0, 149.0, 148.7, 147.2, 141.1, 124.0, 120.6, 107.0, 56.6, 56.1, 50.2, 45.9, 44.8, 41.3, 41.2, 34.8, 34.7, 34.6, 34.5, 32.4, 32.3, 29.6, 28.9, 24.2, 21.3, 19.3 ppm. HRMS *m/z*: C₂₃H₂₆N₆F₃O₂ calc. 491.1835 [M + H]⁺, found 491.2482. HPLC (*t*_R = 11.94 min, 100% - method (B)).

(*R*)-3-Amino-1-((5*R**,9*R**)-1-isopropyl-4,5,5a,8,9,9a-hexahydro-[1,2,4]triazolo[4,3-*a*][1,6]naphthyridin-7(6*H*)-yl)-4-(2,4,5-trifluorophenyl)butan-1-one (**47**, 100% Yield). ¹H NMR (400 MHz, MeOD₄) δ/ppm 7.42–7.36 (m, 1H), 7.27–7.21 (m, 1H), 4.75 (dd, *J* = 14.4, 15.6 Hz, 2H), 4.34–4.26 (m, 1H), 4.10–4.04 (m, 1H), 3.89–3.82 (m, 1H), 3.51–3.43 (m, 1H), 3.27–3.21 (m, 1H), 3.16–3.02 (m, 4H), 2.96–2.64 (m, 4H), 2.13–1.74 (m, 2H), 1.44 (2d, 3H), 1.41 (2d, 3H) ppm. ¹³C NMR (100 MHz, MeOD₄) δ 169.8 (2), 169.6, 161.1, 154.5, 120.6, 107.2, 107.0, 106.8, 61.7, 50.2, 46.1, 44.8, 41.5, 41.2, 41.0, 34.9, 34.8, 32.4, 31.4, 27.8, 23.3, 23.1, 21.2, 20.8 ppm. LC/MS *m/z* 436.2 [M + H]⁺. HPLC (*t*_R = 7.64 min, 100% - method (B)).

4,4-Difluoro-*N*-((*S*)-3-((5*S**,9*R**)-1-methyl-4,5,5a,8,9,9a-hexahydro-[1,2,4]triazolo[4,3-*a*][1,6]naphthyridin-7(6*H*)-yl)-1-phenylpropyl)cyclohexane-1-carboxamide (**48**). To a solution of CBz protected amine **51a** (200 mg, 0.4 mmol, 1 equiv) in methanol (7 mL) was added Pd/C and the reaction was stirred under an atmosphere of hydrogen overnight. The crude product was filtered through Celite and the solvent was evaporated under reduced pressure.

To 4,4-difluorocyclohexane-1-carboxylic acid (38 mg, 0.2 mmol, 1.5 equiv) in DMF (3.5 mL) was added DIPEA (56 μL, 0.3 mmol, 3.0 equiv), HATU (50 mg, 0.13 mmol, 1.2 equiv) and amine (50 mg, 0.15 mmol, 1.0 equiv). The reaction was stirred at RT for 2h. and was diluted with water (10 mL). The aqueous phase was extracted with ethyl acetate (3 × 10 mL) and the combined organic phases were washed with saturated aqueous ammonium chloride (10 mL), dried over Na₂SO₄, filtered and the solvent was evaporated under reduced pressure. The crude product was purified by flash chromatography (dichloromethane/methanol 20:1) to yield amine **48** (68 mg, 33%) as a white solid after further purification using preparative HPLC.

¹H NMR (400 MHz, CDCl₃) δ 7.39–7.26 (m, 5H), 6.37 (dd, *J* = 8.2 Hz, 0.5H), 6.22 (d, *J* = 7.5 Hz, 0.5H), 5.15–5.05 (2q, *J* = 7.55 Hz; *J* = 6.92 Hz, 1H), 4.02–3.96 (m, 1H), 3.26–3.16 (m, 1H), 3.12–3.09 (m, 0.5H), 3.02–2.98 (m, 0.5H), 2.94–2.91 (m, 0.5H), 2.88–2.83 (m, 1.5H), 2.42 (s, Me, 3H), 2.34–2.12 (m, 6H), 2.06–1.76 (m, 13H) ppm. HRMS *m/z* C₂₆H₃₆F₂N₅O calc. 472.2882 [M + H]⁺, found 472.2845. HPLC (*t*_R 12.64 min, 100% - method (B)).

4,4-Difluoro-*N*-((*S*)-3-((5*R**,9*R**)-1-methyl-4,5,5a,8,9,9a-hexahydro[1,2,4]triazolo[4,3-*a*][1,6]naphthyridin-7(6*H*)-yl)-1-phenylpropyl)cyclohexane-1-carboxamide (**49**). To a solution of CBz protected amine **51b** (97 mg, 0.2 mmol, 1.0 equiv) in methanol (1 mL) was added Pd/C and the reaction was stirred under an atmosphere of hydrogen overnight. The crude product was filtered through Celite and the solvent was evaporated under reduced pressure. To difluorocyclohexane-1-carboxylic acid (20 mg, 0.12 mmol, 1.5 equiv) in DMF (2.5 mL) was added DIPEA (33 μL, 0.24 mmol, 3.0 equiv), HATU (37 mg, 0.1 mmol, 1.2eq) and amine (26 mg, 0.1 mmol, 1.0 equiv). The reaction was stirred at rt for 2h and was diluted with water (10 mL). The aqueous phase was extracted with ethyl acetate (3 × 10 mL) and the combined organic phases were washed with saturated aqueous ammonium chloride (10 mL), dried over Na₂SO₄, filtered and the solvent was evaporated under reduced pressure. The crude product was purified by flash chromatography (dichloromethane/methanol 20:1) and SCX column chromatography (dichloromethane to methanol to 7*N* ammonia in methanol) to yield amine **49** (9 mg, 24%) as a white solid after further purification using preparative HPLC.

¹H NMR (400 MHz, CDCl₃) δ 7.36–7.24 (m, 5H), 6.89–6.84 (m, 1H), 5.05 (q, *J* = 7.0 Hz, 1H), 3.55 (t, *J* = 10.8 Hz, 1H), 3.26 (d, *J* = 11.3 Hz, 1H), 3.20–3.15 (m, 2H), 2.92–2.83 (m, 1H), 2.68 (dt, *J* = 2.5, 12.6 Hz, 1H), 2.49 (d, 3H), 2.34–2.24 (m, 1H), 2.22–1.66 (m, 18H), 1.62–1.52 (m, 1H) ppm. ¹³C NMR (100 MHz, CDCl₃) δ 173.6, 151.9, 149.9, 141.4, 128.8, 127.6, 124.4, 120.6, 58.8, 57.4, 54.5, 52.1, 42.9, 40.2, 32.9, 32.6, 32.2, 29.9, 26.0, 25.0, 22.7, 14.1. HRMS *m/z* C₂₆H₃₆NF₂O₂ calc. 472.2882 [M + H]⁺, found 472.2924. HPLC (*t*_R 12.17 min, 98% - method (B)).

rel-(5*R*,9*R*)-1-Methyl-4,5,5a,6,7,8,9,9a-octahydro-[1,2,4]triazolo[4,3-*a*][1,6]naphthyridine (**50**). By the method outline previously, 1-methyl-4,5,5a,6,7,8,9,9a-octahydro-[1,2,4]triazolo[4,3-*a*][1,6]naphthyridine was prepared in 76% yield. ¹H NMR (400 MHz, CDCl₃) δ 3.61 (dt, *J* = 4.2, 11.2 Hz, 1H), 3.26 (m, 1H), 3.18–3.12 (m, 2H), 2.89–2.77 (m, 2H), 2.63–2.54 (m, 2H), 2.48 (s, 3H), 1.87–1.74 (m, 3H), 1.66 (qd, *J* = 3.7, 11.5 Hz, 1H), 1.50 (qd, *J* = 5.2, 12.6 Hz, 1H) ppm. ¹³C NMR (100 MHz, CDCl₃) δ 152.2, 150.0, 59.9, 51.0, 45.4, 42.5, 31.9, 25.0, 23.0, 14.3 (Me) ppm. HRMS *m/z*: C₁₀H₁₇N₄ calculated 193.1448 [M + H]⁺ found 193.1389.

Benzyl ((*S*)-3-((5*S**,9*R**)-1-Methyl-4,5,5a,8,9,9a-hexahydro[1,2,4]triazolo[4,3-*a*][1,6]naphthyridin-7(6*H*)-yl)-1-phenylpropyl)carbamate (**51a**). To a solution of benzyl ((*S*)-3-oxo-1-phenylpropyl)carbamate (530 mg, 1.5 mmol, 1.4 equiv) in 1,2-dichloroethane (6.3 mL) was added sodium triacetoxycborohydride (386 mg, 1.8 mmol, 1.2 equiv) and rel-(5*R*,9*R*)-1-methyl-4,5,5a,6,7,8,9,9a-octahydro-[1,2,4]triazolo[4,3-*a*][1,6]naphthyridine (**50**) (200 mg, 1.0 mmol, 1.7 equiv). The reaction was stirred overnight and the crude reaction mixture was diluted with saturated aqueous sodium bicarbonate (25 mL). The aqueous phase was extracted with ethyl acetate (3 × 25 mL). The combined organic phases were dried over Na₂SO₄, filtered and the solvent was evaporated under reduced pressure. The crude product was purified

by flash chromatography (dichloromethane/methanol, 10:1) to give **51a** (40 mg, 57%) as a colorless oil, which was further purified by preparative HPLC.

HPLC: (t_R = 15.2 min, 97%, method (B)). ^1H NMR (400 MHz, CDCl_3) δ 7.37–7.22 (m, 10H), 7.13 (m, 1H), 5.16–5.03 (m, 1H), 4.96–4.83 (m, 2H), 3.97–3.91 (m, 1H), 3.11–2.53 (m, 4H), 2.40 (s, Me, 4H), 2.39–2.19 (m, 3H), 2.11–1.69 (m, 9H) ppm. ^{13}C NMR (101 MHz, CDCl_3) δ 156.0 (2), 150.4, 149.3, 136.6, 136.5, 128.7 (2), 127.4, 126.2, 67.7, 66.9, 66.8, 54.9, 54.4, 52.1, 42.5, 34.5, 34.0, 32.2, 21.5, 21.2, 19.7, 10.6 ppm. HRMS m/z $\text{C}_{27}\text{H}_{34}\text{N}_5\text{O}_2$ calc. 460.2707 [$\text{M} + \text{H}$] $^+$, found 460.2319.

Benzyl ((S)-3-((5R*,9R*)-1-Methyl-4,5,5a,8,9,9a-hexahydro-[1,2,4]triazolo[4,3-a][1,6]naphthyridin-7(6H)-yl)-1-phenylpropyl)-carbamate (51b). To a solution of benzyl (S)-(3-oxo-1-phenylpropyl)carbamate (331 mg, 0.9 mmol, 1.1 equiv) in 1,2 dichloroethane (5 mL) was added sodium triacetoxymethylborohydride (244 mg, 1.15 mmol), acetic acid (47 μL) and *rel*-(5S,9R)-1-methyl-4,5,5a,6,7,8,9,9a-octahydro-[1,2,4]triazolo[4,3-a][1,6]naphthyridine **24** (170 mg, 0.8 mmol, 1.4 equiv) in 1,2 dichloroethane (2 mL). The reaction was stirred overnight and the crude reaction mixture was diluted with saturated aqueous sodium bicarbonate (10 mL). The aqueous phase was extracted with ethyl acetate (3 \times 25 mL). The combined organic phases were dried over Na_2SO_4 , filtered and the solvent was evaporated. The crude product was purified by flash chromatography (petrol ether/ethyl acetate, 2:1) to give the product **51b** (217 mg, 57%) as colorless oil, which was further purified by preparative HPLC.

HPLC (t_R = 14.41 min, 98%, method (B)). ^1H NMR (400 MHz, CDCl_3) δ 7.36–7.21 (m, 10H), 6.90–6.77 (2 x bs, 1 H), 5.17–5.06 (m, 1H), 5.01–4.93 (m, 1H), 4.90–4.81 (m, 1H), 3.49–3.17 (m, 2H), 3.15–2.86 (m, 3H), 2.78–2.67 (m, 1H), 2.52–2.46 (m, 1H), 2.44 (s, 3H), 2.41–2.30 (m, 2H), 2.14–1.99 (m, 2H), 1.93–1.69 (m, 5H), 1.55–1.42 (m, 1H) ppm. ^{13}C NMR (101 MHz, CDCl_3) δ 155.9, 152.1, 149.9, 136.6, 128.5, 128.3, 127.9, 127.1, 126.1, 66.4, 59.2, 58.9, 57.8, 54.5, 52.3, 51.6, 42.4, 40.8, 40.7, 32.8, 30.5, 30.3, 24.9, 22.6, 14.0 ppm. LCMS m/z $\text{C}_{27}\text{H}_{34}\text{N}_5\text{O}_2$ calc. 460.2707 [$\text{M} + \text{H}$] $^+$ found 460.2 [$\text{M} + \text{H}$] $^+$.

tert-Butyl 4-(3-(Methyl-4H-1,2,4-triazol-4-yl)piperidine-1-carboxylate (53). Acetic hydrazide (0.814 g) was dissolved in acetonitrile (2 mL) and dimethylformamide dimethyl acetal (1.31 g) was added. The mixture was heated to 50 $^\circ\text{C}$ for 30 min and then *N*-1 *boc*-4-aminopiperidine (1.00 g) was added followed by acetic acid (1 mL). The reaction was heated to 100 $^\circ\text{C}$ for 20 h and was cooled and concentrated. The residue was partitioned between ethyl acetate (20 mL) and saturated sodium bicarbonate (20 mL) and was extracted into ethyl acetate (2 \times 20 mL). The combined extracts were dried (MgSO_4), filtered and concentrated. The residue was purified by chromatography on silica gel eluting with 0.7 N ammonia in methanol in dichloromethane (1/9) to give the product (1.15 g, 86%) as an oil.

^1H NMR (400 MHz, CDCl_3) δ = 8.13 (s, 1H); 4.42–4.26 (m, 2H); 4.03–3.95 (m, 1H); 2.91–2.80 (m, 2H); 2.49 (s, 3H); 2.06–1.99 (m, 2H); 2.00 (dq, J = 4.4 and 12.3 Hz, 2H); 1.48 (s, 9H) ppm. ^{13}C NMR (101 MHz, CDCl_3) δ = 154.4, 150.0, 140.97, 80.4, 53.45, 53.29, 32.81, 28.41, 10.73 ppm. LRMS (m/z) calcd. for $\text{C}_{13}\text{H}_{22}\text{N}_4\text{O}_2$ [$\text{M} + \text{H}$] $^+$ 267.2, found 267.1.

tert-Butyl 4-(3-(Trifluoromethyl)-4H-1,2,4-triazol-4-yl)piperidine-1-carboxylate (54, 43% Yield). ^1H NMR (400 MHz, CDCl_3) δ = 8.37 (s, 1H), 4.46–4.34 (m, 2H), 4.33 (tt, J 12.5 and 4.0 Hz, 1H), 2.94–2.82 (m, 2H), 2.22–2.08 (m, 2H), 1.87 (dq, J 12.5 and 4.0 Hz, 2H), 1.51 (s, 9H), LRMS (m/z): calcd. for $\text{C}_{25}\text{H}_{29}\text{N}_5\text{O}_3\text{S}$ [$\text{M} + \text{H}$] $^+$ 480.6, found 480.3.

General Procedure for Reductive Amination Reaction. A stirred solution of 2-chloro-4-morpholinethieno[3,2-*d*]pyrimidine-6-carbaldehyde (1.1 mmol, 1.1 equiv) and corresponding substituted piperidine (e.g., **24**, 1 mmol, 1 equiv) in methanol (9 mL) and acetic acid (1 mL) was heated to 40 $^\circ\text{C}$ for 1 h. and cooled to room temperature where picoline borane (1.5 mmol, 1.5 equiv) was added and the resulting reaction was stirred at room temperature for 20 h. The reaction mixture was concentrated and partitioned between dichloromethane (10 mL) and saturated sodium hydrogen carbonate (10 mL). The

mixture was extracted with dichloromethane (2 \times 15 mL) and the combined extracts were dried (MgSO_4), filtered and concentrated. The residue was purified by chromatography on silica gel eluting with 2 to 10% methanol (containing 0.7N ammonia) in dichloromethane to afford the product.

4-(2-Chloro-6-((4-(3-methyl-4H-1,2,4-triazol-4-yl)piperidin-1-yl)methyl)thieno[3,2-*d*]pyrimidin-4-yl)morpholine (56, Yield 71%). ^1H NMR (400 MHz, DMSO) δ 8.61 (s, 1H), 7.33 (s, 1H), 4.07–3.94 (m, 1H), 3.96–3.87 (m, 6H), 3.81–3.73 (m, 4H), 3.06–2.99 (m, 2H), 2.38 (s, 3H), 2.31–2.26 (m, 2H), 1.97–1.84 (m, 4H), LRMS (m/z) calcd. for $\text{C}_{19}\text{H}_{24}\text{ClN}_7\text{OS}$ [$\text{M} + \text{H}$] $^+$ 434.0, found 434.4.

4-(2-Chloro-6-((4-(3-(trifluoromethyl)-4H-1,2,4-triazol-4-yl)piperidin-1-yl)methyl)thieno[3,2-*d*]pyrimidin-4-yl)morpholine (57, Yield 30%). ^1H NMR (400 MHz, DMSO) δ 9.26 (s, 1H), 7.32 (s, 1H), 4.26–4.13 (m, 1H), 3.93 (s, 2H), 3.92–3.87 (m, 4H), 3.81–3.74 (m, 4H), 3.08–3.00 (m, 2H), 2.31 (td, J = 2.5, 11.8 Hz, 2H), 2.09 (qd, J = 3.6, 12.0 Hz, 2H), 2.04–1.96 (m, 2H). ^{13}C NMR (101 MHz, DMSO) δ 163.0, 158.4, 156.3, 152.9, 145.8, 142.6, 122.4, 117.9, 112.7, 66.3, 56.4, 54.9, 52.2, 46.4, 39.9, 32.8. LRMS (m/z): calcd. for $\text{C}_{19}\text{H}_{21}\text{ClF}_3\text{N}_7\text{OS}$ [$\text{M} + \text{H}$] $^+$ 488.9, found 488.3.

rel-4-(2-Chloro-6-(((5S,9R)-1-methyl-4,5,5a,8,9,9a-hexahydro-[1,2,4]triazolo[4,3-a][1,6]naphthyridin-7(6H)-yl)methyl)thieno[3,2-*d*]pyrimidin-4-yl)morpholine (58, Yield 49%). ^1H NMR (400 MHz, CDCl_3) δ 7.21 (s, 1H), 4.15 (dt, J = 5.1 and 11.6 Hz, 1H), 4.06–3.98 (m, 4H), 3.91–3.79 (m, 6H), 3.30 (dd, J = 5.6 and 17.5 Hz, 1H), 3.11–3.03 (m, 2H), 2.95–2.85 (m, 1H), 2.57–2.43 (m, 2H), 2.51 (s, 3H), 2.32–2.26 (m, 2H), 2.05–1.97 (m, 1H), 1.96–1.87 (m, 2H) ppm. LRMS (m/z) calcd. for $\text{C}_{21}\text{H}_{26}\text{ClN}_7\text{OS}$ [$\text{M} + \text{H}$] $^+$ 460.2, found 460.4.

rel-4-(2-Chloro-6-(((5S,9R)-1-(trifluoromethyl)-4,5,5a,8,9,9a-hexahydro[1,2,4]triazolo[4,3-a][1,6]naphthyridin-7(6H)-yl)methyl)thieno[3,2-*d*]pyrimidin-4-yl)morpholine (59, Yield 91%). ^1H NMR (400 MHz, CDCl_3) δ 7.34 (s, 1H), 4.53–4.43 (m, 1H), 4.08–3.99 (m, 4H), 3.91–3.85 (m, 6H), 3.42–3.33 (m, 1H), 3.31–3.18 (m, 1H), 3.04–2.91 (m, 1H), 2.84–2.66 (m, 2H), 2.44–2.34 (m, 2H), 2.28–2.21 (m, 2H), 2.03–1.97 (m, 2H) ppm. LRMS (m/z) calcd. for $\text{C}_{21}\text{H}_{23}\text{ClF}_3\text{N}_7\text{OS}$ [$\text{M} + \text{H}$] $^+$ 514.13, found 514.2.

rel-4-(2-Chloro-6-(((5R,9R)-1-methyl-4,5,5a,8,9,9a-hexahydro-[1,2,4]triazolo[4,3-a][1,6]naphthyridin-7(6H)-yl)methyl)thieno[3,2-*d*]pyrimidin-4-yl)morpholine (60, Yield 54%). ^1H NMR (400 MHz, DMSO) δ 7.32 (s, 1H), 4.20–3.62 (m, 10H), 2.98–2.86 (m, 3H), 2.64–2.55 (m, 3H), 2.40 (s, 3H), 1.79–1.63 (m, 2H), 1.58–1.43 (m, 4H), LRMS (m/z) calcd. for $\text{C}_{21}\text{H}_{26}\text{ClN}_7\text{OS}$ [$\text{M} + \text{H}$] $^+$ 460.5, found 460.3.

rel-4-(2-Chloro-6-(((5R,9R)-1-(trifluoromethyl)-4,5,5a,8,9,9a-hexahydro-[1,2,4]triazolo[4,3-a][1,6]naphthyridin-7(6H)-yl)methyl)thieno[3,2-*d*]pyrimidin-4-yl)morpholine (61, Yield 62%). ^1H NMR (400 MHz, DMSO) δ 7.32 (s, 1H), 4.03–3.85 (m, 7H), 3.78–3.72 (m, 4H), 3.15–3.00 (m, 3H), 3.02–2.88 (m, 1H), 2.41–2.29 (m, 2H), 2.20–1.98 (m, 2H), 1.95–1.73 (m, 2H), 1.67–1.52 (m, 1H), LRMS (m/z) calcd. for $\text{C}_{21}\text{H}_{23}\text{ClF}_3\text{N}_7\text{OS}$ [$\text{M} + \text{H}$] $^+$ 514.5, found 514.4.

General Procedure for Suzuki Reaction. A mixture of the chlorinated pyrimidine (**56-61**) (0.17 mmol, 1 equiv), aryl boronic acid (**40**), (0.25 mmol, 1.5 equiv), aqueous 2 M Na_2CO_3 (0.51 mmol, 3 equiv) and *bis*(triphenylphosphine) palladium chloride (0.017 mmol, 0.1 equiv) in EtOH: deionized water, (3 mL, 3:1) was irradiated under microwave radiation for 45 min at 125 $^\circ\text{C}$. After concentration the residue was purified by flash column chromatography (silica gel), eluting with 0–10% MeOH in CH_2Cl_2 containing NH_3 (0.7 N) to give the product.

3-(6-((4-(3-Methyl-4H-1,2,4-triazol-4-yl)piperidin-1-yl)methyl)-4-morpholinethieno[3,2-*d*]pyrimidin-2-yl)phenol (62, Yield 54%). ^1H NMR (400 MHz, DMSO) δ 9.51 (s, 1H), 8.62 (s, 1H), 7.89–7.82 (m, 2H), 7.41 (s, 1H), 7.28 (t, J = 8.0 Hz, 1H), 6.91–6.83 (m, 1H), 4.03–3.96 (m, 5H), 3.94 (s, 2H), 3.86–3.79 (m, 4H), 3.09–3.01 (m, 2H), 2.38 (s, 3H), 2.31–2.26 (m, 2H), 1.98–1.89 (m, 4H). ^{13}C NMR (101 MHz, DMSO) δ 162.7, 159.6, 157.9, 157.9, 150.9, 150.1, 141.7, 139.9, 129.7, 123.6, 119.0, 117.5, 114.9, 112.7, 66.5, 56.8, 52.5, 52.4, 46.3, 32.5, 10.5. LRMS (t_R = 1.98 min, 99% - method (A)), (m/z) calcd. for $\text{C}_{25}\text{H}_{29}\text{N}_7\text{O}_2\text{S}$ [$\text{M} + \text{H}$] $^+$ 492.2, found 492.4.

4-(2-(1*H*-Indazol-4-yl)-6-((4-(3-methyl-4*H*-1,2,4-triazol-4-yl)-piperidin-1-yl)methyl)thieno[3,2-*d*]pyrimidin-4-yl)morpholine (**63**, Yield 54%). ¹H NMR (400 MHz, DMSO) δ 13.21 (s, 1H), 8.91 (s, 1H), 8.62 (s, 1H), 8.25 (d, *J* = 7.2 Hz, 1H), 7.68 (d, *J* = 8.2 Hz, 1H), 7.54 (s, 1H), 7.49 (t, *J* = 7.8 Hz, 1H), 4.07–4.00 (m, 5H), 3.97 (s, 2H), 3.90–3.82 (m, 4H), 3.11–3.02 (m, 2H), 2.38 (s, 3H), 2.35–2.22 (m, 2H), 2.01–1.88 (m, 4H). ¹³C NMR (101 MHz, DMSO) δ 162.7, 160.1, 158.1, 151.0, 150.1, 141.7, 141.3, 135.6, 131.6, 126.1, 123.9, 121.7, 121.5, 112.8, 112.6, 66.5, 56.8, 52.5, 52.4, 46.6, 32.6, 10.5. LRMS (*t_R* = 1.99 min, 99% - method (A)), (*m/z*) calcd. for C₂₆H₂₉N₉OS [M + H]⁺ 516.2, found 516.5.

4-(2-(1*H*-Indol-4-yl)-6-((4-(3-methyl-4*H*-1,2,4-triazol-4-yl)-piperidin-1-yl)methyl)thieno[3,2-*d*]pyrimidin-4-yl)morpholine (**64**, Yield 64%). ¹H NMR (400 MHz, DMSO) δ 11.25 (s, 1H), 8.63 (s, 1H), 8.18–8.12 (m, 1H), 7.61–7.40 (m, 3H), 7.26–7.18 (m, 1H), 4.04–3.99 (m, 5H), 3.99–3.94 (m, 2H), 3.92–3.79 (m, 4H), 3.07 (d, *J* = 11.2 Hz, 2H), 2.39 (s, 3H), 2.30 (s, 2H), 1.95 (s, 4H). ¹³C NMR (101 MHz, DMSO) δ 162.8, 161.7, 158.0, 150.5, 150.1, 141.7, 137.5, 130.2, 126.8, 126.4, 123.9, 120.9, 113.8, 112.1, 103.9, 66.5, 56.8, 52.5, 52.4, 46.6, 32.6, 10.5. LRMS (*t_R* = 2.07 min, 99% - method (A)), (*m/z*) calcd. for C₂₇H₃₀N₈O₂S [M + H]⁺ 515.2, found 515.3.

3-(4-Morpholino-6-((4-(3-(trifluoromethyl)-4*H*-1,2,4-triazol-4-yl)-piperidin-1-yl)methyl)thieno[3,2-*d*]pyrimidin-2-yl)phenol (**65**, 89% Yield). ¹H NMR (400 MHz, DMSO) δ 9.50 (s, 1H), 9.27 (s, 1H), 7.85 (d, *J* = 7.1 Hz, 2H), 7.41 (s, 1H), 7.28 (t, *J* = 8.0 Hz, 1H), 6.90–6.83 (m, 1H), 4.23–4.18 (m, 1H), 4.02–3.97 (m, 4H), 3.96–3.92 (m, 2H), 3.86–3.79 (m, 4H), 3.11–3.03 (m, 2H), 2.31 (t, *J* = 11.6 Hz, 2H), 2.12 (dt, *J* = 6.7, 12.4 Hz, 2H), 2.05–2.00 (m, 2H). ¹³C NMR (101 MHz, DMSO) δ 162.7, 159.6, 157.9, 150.9, 145.8, 139.9, 129.7, 123.6, 66.5, 56.6, 55.0, 52.2, 46.3, 32.8. LRMS (*t_R* = 2.18 min, 99% - method (A)), (*m/z*): calcd. for C₂₅H₂₆F₃N₇O₂S [M + H]⁺ 546.6, found 546.4.

4-(2-(1*H*-Indazol-4-yl)-6-((4-(3-(trifluoromethyl)-4*H*-1,2,4-triazol-4-yl)piperidin-1-yl)methyl)thieno[3,2-*d*]pyrimidin-4-yl)morpholine (**66**, 86% Yield). ¹H NMR (400 MHz, DMSO) δ 13.21 (s, 1H), 9.28 (s, 1H), 8.90 (s, 1H), 8.24 (d, *J* = 7.3 Hz, 1H), 7.68 (d, *J* = 8.3 Hz, 1H), 7.53 (s, 1H), 7.48 (t, *J* = 7.8 Hz, 1H), 4.27–4.19 (m, 1H), 4.03 (t, *J* = 4.7 Hz, 4H), 3.99–3.94 (m, 2H), 3.90–3.82 (m, 4H), 3.10 (d, *J* = 11.4 Hz, 2H), 2.33 (t, *J* = 11.5 Hz, 2H), 2.17–2.09 (m, 2H), 2.07–2.02 (m, 2H). LRMS (*t_R* = 2.25 min, 97% - method (A)), (*m/z*): calcd. for C₂₇H₂₇F₃N₈O₂S [M + H]⁺ 569.6, found 569.4.

4-(2-(1*H*-Indol-4-yl)-6-((4-(3-methyl-4*H*-1,2,4-triazol-4-yl)-piperidin-1-yl)methyl)thieno[3,2-*d*]pyrimidin-4-yl)morpholine (**67**, 97% Yield). ¹H NMR (400 MHz, DMSO) δ 11.24 (s, 1H), 9.28 (s, 1H), 8.14 (d, *J* = 7.5 Hz, 1H), 7.53 (d, *J* = 8.0 Hz, 1H), 7.49–7.43 (m, 1H), 7.21 (t, *J* = 7.7 Hz, 1H), 4.26–4.15 (m, 1H), 4.05–3.99 (m, 4H), 3.98–3.93 (m, 2H), 3.88–3.81 (m, 4H), 3.16–3.05 (m, 2H), 2.32 (t, *J* = 11.5 Hz, 2H), 2.19–2.05 (m, 2H), 2.06–2.01 (m, 2H). ¹³C NMR (101 MHz, DMSO) δ 162.8, 161.8, 158.0, 150.6, 145.8, 142.8 (q, *J* = 76.9 Hz), 137.5, 130.2, 126.8, 126.4, 123.9, 120.9, 119.2 (q, *J* = 269.3, 297.5 Hz), 113.8, 112.1, 103.9, 66.5, 56.6, 55.0, 52.2, 46.5, 32.9. LRMS (*t_R* = 2.19 min, 99% - method (A)), (*m/z*): calcd. for C₂₇H₂₇F₃N₈O₂S [M + H]⁺ 569.6, found 569.4.

rel-4-(2-(1*H*-Indazol-4-yl)-6-(((5*S*,9*R*)-1-(trifluoromethyl)-4,5,5*a*,8,9,9*a*-hexahydro[1,2,4]triazolo[4,3-*a*][1,6]naphthyridin-7(6*H*)-yl)methyl)thieno[3,2-*d*]pyrimidin-4-yl)morpholine (**68**, 65% Yield). ¹H NMR (400 MHz, *d*₆-DMSO) δ = 13.21 (s, 1H), 8.90 (s, 1H), 8.24 (d, *J* = 7 Hz, 1H), 7.68 (d, *J* = 8.1 Hz, 1H), 7.51 (s, 1H), 7.49 (t, *J* = 7.8 Hz, 1H), 4.51–4.46 (m, 1H), 4.06–3.99 (m, 4H), 3.90 (q, *J* = 15 Hz, 2H), 3.89–3.82 (m, 4H), 3.17 (dd, *J* = 16 and 5.9 Hz, 1H), 3.05–2.97 (m, 2H), 2.94–2.85 (m, 1H), 2.50–2.41 (m, 1H), 2.36–2.24 (m, 2H), 2.08–1.92 (m, 2H), 1.87–1.79 (m, 1H) ppm. ¹³C NMR (101 MHz, *d*₆-DMSO) δ 162.8, 160.1, 158.1, 154.2, 151.3, 142.2 (d, *J*_{C-F} = 38.5 Hz), 141.2, 135.6, 131.6, 126.1, 123.6, 121.6, 121.5, 119.3 (d, *J*_{C-F} = 269 Hz), 112.8, 112.5, 66.5, 56.8, 56.6, 54.2, 52.1, 46.6, 33.6, 29.6, 21.3, 20.1 ppm. LRMS (*t_R* = 2.40 min, 98% - method (A)), (*m/z*) calcd. for C₂₈H₂₈F₃N₉O₂S [M + H]⁺ 596.65, found 596.4.

rel-3-(4-Morpholino-6-(((5*S*,9*R*)-1-(trifluoromethyl)-4,5,5*a*,8,9,9*a*-hexahydro[1,2,4]triazolo[4,3-*a*][1,6]naphthyridin-7(6*H*)-yl)methyl)thieno[3,2-*d*]pyrimidin-2-yl)phenol (**69**, 72% Yield). ¹H NMR (400 MHz, DMSO) δ = 9.49 (s, 1H), 7.87–7.83 (m, 2H), 7.39 (s, 1H), 7.28 (t, *J* = 8.2 Hz), 6.87 (d, *J* = 9 Hz, 1H), 4.51–4.45 (m, 1H), 4.07–

3.96 (m, 4H), 3.87 (q, *J* = 15 Hz, 2H), 3.85–3.79 (m, 4H), 3.21–3.13 (m, 1H), 3.02–2.96 (m, 2H), 2.94–2.85 (m, 1H), 2.50–2.40 (m, 1H), 2.35–2.23 (m, 2H), 2.07–1.91 (m, 2H), 1.85–1.78 (m, 1H) ppm. ¹³C NMR (101 MHz, *d*₆-DMSO) δ 162.8, 159.5, 157.9, 154.2, 151.2, 142.2 (d, *J*_{C-F} = 38.5 Hz), 139.9, 129.7, 123.3, 119.3 (d, *J*_{C-F} = 269 Hz), 119.0, 118.0, 117.5, 114.9, 112.7, 66.5, 56.8, 56.6, 54.2, 52.1, 46.4, 33.5, 29.6, 21.3, 20.1 ppm. LRMS (*t_R* = 2.36 min, 98% - method (A)), (*m/z*) calcd. for C₂₇H₂₈F₃N₇O₂S [M + H]⁺ 572.2, found 572.2.

rel-3-(6-(((5*S*,9*R*)-1-Methyl-4,5,5*a*,8,9,9*a*-hexahydro[1,2,4]triazolo[4,3-*a*][1,6]naphthyridin-7(6*H*)-yl)methyl)-4-morpholinothieno[3,2-*d*]pyrimidin-2-yl)phenol (**70**, 95% Yield). ¹H NMR (400 MHz, DMSO) δ = 9.52 (s, 1H), 7.85–7.84 (m, 2H), 7.38 (s, 1H), 7.28 (t, *J* = 7.7 Hz, 1H), 6.87 (d, *J* = 7.7 Hz, 1H), 4.24–4.16 (m, 1H), 4.05–3.96 (m, 4H), 3.87 (q, *J* = 15 Hz, 2H), 3.84–3.79 (m, 4H), 3.03–2.92 (m, 3H), 2.74–2.63 (m, 1H), 2.44–2.39 (m, 1H), 2.38–2.28 (m, 1H), 2.32 (s, 3H), 2.34 (t, *J* = 12 Hz, 1H), 2.19–2.11 (m, 1H), 1.99–1.93 (m, 1H), 1.79–1.65 (m, 2H) ppm. ¹³C NMR (101 MHz, *d*₆-DMSO) δ 162.8, 159.5, 157.9 (2 x C), 151.4, 149.9, 149.2, 140.0, 129.8, 123.3, 119.1, 117.6, 115.0, 112.7, 66.5, 57.2, 57.0, 52.3, 51.3, 46.4, 34.2, 28.9, 21.5, 21.0, 10.4 ppm. LRMS (*t_R* = 2.02 min, 99% - method (A)), (*m/z*) calcd. for C₂₇H₃₁N₇O₂S [M + H]⁺ 518.65, found 518.5.

rel-4-(2-(1*H*-Indazol-4-yl)-6-(((5*S*,9*R*)-1-methyl-4,5,5*a*,8,9,9*a*-hexahydro[1,2,4]triazolo[4,3-*a*][1,6]naphthyridin-7(6*H*)-yl)methyl)thieno[3,2-*d*]pyrimidin-4-yl)morpholine (**71**, 68% Yield). ¹H NMR (400 MHz, DMSO) δ = 13.22 (s, 1H), 8.90 (s, 1H), 8.24 (d, *J* = 7.3 Hz, 1H), 7.68 (d, *J* = 7.7 Hz, 1H), 7.52–7.46 (m, 2H), 4.25–4.18 (m, 1H), 4.06–4.0 (m, 4H), 3.90 (q, *J* = 15 Hz, 2H), 3.89–3.82 (m, 4H), 3.05–2.93 (m, 3H), 2.75–2.64 (m, 1H), 2.47–2.41 (m, 1H), 2.38–2.28 (m, 1H), 2.32 (s, 3H), 2.25 (t, *J* = 11 Hz, 1H), 2.19–2.11 (m, 1H), 2.01–1.94 (m, 1H), 1.80–1.66 (m, 2H) ppm. ¹³C NMR (101 MHz, *d*₆-DMSO) δ 162.8, 160.1, 158.1, 151.4, 149.9, 149.1, 141.3, 135.6, 131.6, 126.1, 123.5, 121.6, 121.5, 112.8, 112.5, 66.5, 57.2, 57.0, 52.3, 51.3, 46.6, 34.2, 28.9, 21.5, 20.9, 10.4 ppm. LRMS (*m/z*) (*t_R* = 2.04 min, 98% - method (A)), calcd. for C₂₇H₃₁N₉O₂S [M + H]⁺ 542.68, found 542.4.

rel-4-(2-(1*H*-Indol-4-yl)-6-(((5*S*,9*R*)-1-(trifluoromethyl)-4,5,5*a*,8,9,9*a*-hexahydro[1,2,4]triazolo[4,3-*a*][1,6]naphthyridin-7(6*H*)-yl)methyl)thieno[3,2-*d*]pyrimidin-4-yl)morpholine (**72**, 62% Yield). ¹H NMR (400 MHz, DMSO) δ 11.24 (s, 1H), 8.14 (d, *J* = 7.4 Hz, 1H), 7.53 (d, *J* = 8.0 Hz, 1H), 7.46 (s, 3H), 7.21 (t, *J* = 7.8 Hz, 1H), 5.77 (s, 1H), 4.03–3.96 (m, 4H), 3.87–3.79 (m, 4H), 3.34 (s, 1H), 3.19–3.02 (m, 3H), 2.95 (ddd, *J* = 6.2, 11.4, 17.3 Hz, 1H), 2.41–2.29 (m, 2H), 2.18–2.02 (m, 2H), 1.92–1.74 (m, 2H), 1.59 (tt, *J* = 6.7, 13.5 Hz, 1H). ¹³C NMR (101 MHz, DMSO) δ 162.8, 161.7, 158.0, 156.1, 150.4, 137.5, 130.2, 126.8, 126.4, 123.9, 120.9, 113.8, 112.1, 110.0, 103.9, 66.5, 60.5, 57.0, 56.4, 55.4, 51.9, 46.5, 30.5, 23.4, 22.7. LRMS (*t_R* = 2.33 min, 97% - method (A)), (*m/z*): calcd. for C₂₉H₂₉F₃N₈O₂S [M + H]⁺ 595.7, found 595.5.

rel-4-(2-(1*H*-Indol-4-yl)-6-(((5*S*,9*R*)-1-methyl-4,5,5*a*,8,9,9*a*-hexahydro[1,2,4]triazolo[4,3-*a*][1,6]naphthyridin-7(6*H*)-yl)methyl)thieno[3,2-*d*]pyrimidin-4-yl)morpholine (**73**, 60% Yield). ¹H NMR (400 MHz, DMSO) δ = 11.24 (s, 1H), 8.14 (d, *J* = 7.0 Hz, 1H), 7.53 (d, *J* = 8.1 Hz, 1H), 7.47–7.43 (m, 3H), 7.21 (t, *J* = 8.1 Hz), 4.21–4.17 (m, 1H), 4.0–4.0 (m, 4H), 3.88 (q, *J* = 15 Hz, 2H), 3.87–3.81 (m, 4H), 3.04–2.93 (m, 3H), 2.74–2.64 (m, 1H), 2.45–2.39 (m, 1H), 2.37–2.29 (m, 1H), 2.32 (s, 3H), 2.24 (t, *J* = 10.9 Hz, 1H), 2.17–2.11 (m, 1H), 2.01–1.94 (m, 1H), 1.79–1.65 (m, 2H) ppm. ¹³C NMR (101 MHz, *d*₆-DMSO) δ 162.9, 161.7, 158.0, 150.9, 149.9, 149.1, 137.5, 130.2, 126.8, 126.4, 123.6, 120.9, 120.8, 113.8, 112.1, 103.8, 66.5, 65.4, 57.1, 57.0, 52.2, 51.4, 46.6, 34.1, 28.9, 21.5, 21.0, 10.4 ppm. LRMS (*t_R* = 2.03 min, 98% - method (A)), (*m/z*) calcd. for C₂₉H₃₂N₈O₂S [M + H]⁺ 541.69, found 541.3.

rel-4-(2-(1*H*-Indazol-4-yl)-6-(((5*R*,9*R*)-1-(trifluoromethyl)-4,5,5*a*,8,9,9*a*-hexahydro[1,2,4]triazolo[4,3-*a*][1,6]naphthyridin-7(6*H*)-yl)methyl)thieno[3,2-*d*]pyrimidin-4-yl)morpholine (**74**, 78% Yield). ¹H NMR (400 MHz, DMSO) δ 11.24 (s, 1H), 8.14 (d, *J* = 7.4 Hz, 1H), 7.53 (d, *J* = 8.0 Hz, 1H), 7.48–7.43 (m, 3H), 7.21 (t, *J* = 7.8 Hz, 1H), 5.77 (s, 1H), 4.03–3.96 (m, 4H), 3.97–3.91 (m, 2H), 3.87–3.79 (m, 4H), 3.19–3.06 (m, 2H), 3.08–2.91 (m, 2H), 2.35 (t, *J* = 12.2 Hz, 2H), 2.10 (p, *J* = 11.1 Hz, 2H), 1.83 (ddt, *J* = 7.3, 13.8, 27.0

H_z, 2H), 1.59 (tt, *J* = 6.7, 13.5 Hz, 1H). LRMS (*t_R* = 2.28 min, 99% - method (A)), (*m/z*): calcd. for C₂₇H₂₈F₃N₇O₂S [M + H]⁺ 572.6, found 572.4.

*rel-3-(4-Morpholino-6-(((5R,9R)-1-(trifluoromethyl)-4,5,5a,8,9,9a-hexahydro[1,2,4]triazolo[4,3-*a*][1,6]naphthyridin-7(6H)-yl)methyl)thieno[3,2-*d*]pyrimidin-2-yl)phenol (75, 74% Yield)*. ¹H NMR (400 MHz, DMSO) δ 9.50 (s, 1H), 7.89–7.82 (m, 2H), 7.40 (s, 1H), 7.28 (t, *J* = 8.0 Hz, 1H), 6.91–6.83 (m, 1H), 4.01–3.95 (m, 5H), 3.93 (s, 2H), 3.81 (t, *J* = 4.7 Hz, 4H), 3.18–3.02 (m, 3H), 2.95 (td, *J* = 5.9, 14.5, 16.9 Hz, 1H), 2.37 (d, *J* = 12.1 Hz, 2H), 2.19–2.02 (m, 2H), 1.81 (ddd, *J* = 4.6, 12.3, 24.5 Hz, 2H), 1.60 (tt, *J* = 6.5, 13.6 Hz, 1H). ¹³C NMR (101 MHz, DMSO) 162.7, 159.5, 157.9, 157.9, 156.1, 150.8, 139.9, 129.7, 123.6, 119.0, 117.5, 114.9, 112.7, 66.5, 60.5, 57.0, 56.4, 51.9, 46.3, 39.5, 30.5, 23.4, 22.7. LRMS (*t_R* = 2.23 min, 99% - method (A)), (*m/z*): calcd. for C₂₇H₂₈F₃N₇O₂S [M + H]⁺ 572.6, found 572.4.

*rel-4-(2-(1H-Indazol-4-yl)-6-(((5R,9R)-1-methyl-4,5,5a,8,9,9a-hexahydro[1,2,4]triazolo[4,3-*a*][1,6]naphthyridin-7(6H)-yl)methyl)thieno[3,2-*d*]pyrimidin-4-yl)morpholine (76, 64% Yield)*. ¹H NMR (400 MHz, DMSO) δ 13.21 (s, 1H), 8.91 (s, 1H), 8.25 (d, *J* = 7.2 Hz, 1H), 7.68 (d, *J* = 8.3 Hz, 1H), 7.54 (s, 1H), 7.49 (t, *J* = 7.8 Hz, 1H), 4.06–3.91 (m, 5H), 3.88–3.81 (m, 4H), 3.72 (td, *J* = 3.7, 11.1 Hz, 1H), 3.10 (dd, *J* = 11.3, 24.6 Hz, 2H), 2.92 (dd, *J* = 5.0, 15.9 Hz, 2H), 2.87–2.73 (m, 1H), 2.63–2.58 (m, 1H), 2.42 (s, 3H), 2.39–2.31 (m, 1H), 2.12 (t, *J* = 11.0 Hz, 1H), 1.99–1.85 (m, 1H), 1.83–1.66 (m, 2H), 1.58–1.43 (m, 1H). LRMS (*t_R* = 2.01 min, 99% - method (A)), (*m/z*) calcd. for C₂₈H₃₁N₉O₅ [M + H]⁺ 542.2, found 542.3.

*rel-4-(2-(1H-Indol-4-yl)-6-(((5R,9R)-1-(trifluoromethyl)-4,5,5a,8,9,9a-hexahydro[1,2,4]triazolo[4,3-*a*][1,6]naphthyridin-7(6H)-yl)methyl)thieno[3,2-*d*]pyrimidin-4-yl)morpholine (77, 81% Yield)*. ¹H NMR (400 MHz, DMSO) δ 11.24 (s, 1H), 8.14 (d, *J* = 7.4 Hz, 1H), 7.53 (d, *J* = 8.0 Hz, 1H), 7.48–7.43 (m, 3H), 7.21 (t, *J* = 7.8 Hz, 1H), 5.77 (s, 1H), 4.03–3.96 (m, 4H), 3.97–3.91 (m, 2H), 3.87–3.79 (m, 4H), 3.19–3.06 (m, 2H), 3.08–2.91 (m, 2H), 2.35 (t, *J* = 12.2 Hz, 2H), 2.10 (p, *J* = 11.1 Hz, 2H), 1.83 (ddt, *J* = 7.3, 13.8, 27.0 Hz, 2H), 1.59 (tt, *J* = 6.7, 13.5 Hz, 1H). LRMS (*t_R* = 2.22 min, 99% - method (A)), (*m/z*): calcd. for C₂₇H₂₈F₃N₇O₂S [M + H]⁺ 572.6, found 572.4.

*rel-4-(2-(1H-Indol-4-yl)-6-(((5R,9R)-1-methyl-4,5,5a,8,9,9a-hexahydro[1,2,4]triazolo[4,3-*a*][1,6]naphthyridin-7(6H)-yl)methyl)thieno[3,2-*d*]pyrimidin-4-yl)morpholine (78, Yield 58%)*. ¹H NMR (400 MHz, DMSO) δ 11.25 (s, 1H), 8.18–8.11 (m, 1H), 7.58–7.51 (m, 1H), 7.50–7.43 (m, 3H), 7.26–7.17 (m, 1H), 4.03–3.94 (m, 6H), 3.88–3.81 (m, 4H), 3.76–3.68 (m, 1H), 3.17–3.02 (m, 2H), 2.97–2.88 (m, 1H), 2.83–2.78 (m, 2H), 2.73–2.57 (m, 1H), 2.42 (s, 3H), 2.38–2.33 (m, 1H), 2.16–2.06 (m, 1H), 1.95–1.88 (m, 1H), 1.84–1.65 (m, 1H), 1.55–1.50 (m, 1H). ¹³C NMR (101 MHz, DMSO) δ 162.8, 161.7, 158.0, 151.9, 149.8, 137.5, 130.1, 126.8, 126.4, 123.9, 120.9, 113.8, 112.1, 103.9, 66.5, 58.7, 57.2, 56.6, 52.0, 46.6, 40.7, 40.5, 30.2, 24.8, 22.6, 13.9. LRMS (*t_R* = 2.05 min, 99% - method (A)), (*m/z*) calcd. for C₂₉H₃₂N₈O₅ [M + H]⁺ 541.2, found 541.4.

*rel-3-(6-(((5R,9R)-1-Methyl-4,5,5a,8,9,9a-hexahydro[1,2,4]triazolo[4,3-*a*][1,6]naphthyridin-7(6H)-yl)methyl)-4-morpholiniothieno[3,2-*d*]pyrimidin-2-yl)phenol (79, Yield 59%)*. ¹H NMR (400 MHz, DMSO) δ 9.99–9.42 (m, 1H), 8.11 (s, 1H), 7.94–7.84 (m, 2H), 7.36 (t, *J* = 7.9 Hz, 1H), 7.05–6.98 (m, 1H), 4.97–4.64 (m, 2H), 4.33–4.20 (m, 1H), 4.15–4.08 (m, 4H), 3.90–3.83 (m, 4H), 3.80–2.75 (m, 8H), 2.70 (s, 3H), 2.43–1.88 (m, 2H), 1.76–1.55 (m, 1H). LRMS (*t_R* = 1.97 min, 99% - method (A)), (*m/z*) calcd. for C₂₇H₃₁N₇O₂S [M + H]⁺ 518.2, found 518.6.

Pharmacology—General Methods. DPP-4 Biochemical Assay:⁶³ Enzyme: DPP4 recombinant human protein was purchased from Sino Biological Inc. Substrate: H-Gly-Pro-AMC was purchased from Bachem Americas, Inc. Assay buffer (100 mM Hepes, pH 7.5) was prepared by HitGen. All chemical reagents used were of analytical reagent grade. Assay protocol: Prepare 10 mM compound stock solution in DMSO. The initial rate of DPP4 activity is measured over 15 min by monitoring the fluorescent change (ex/em = 360/460 nm). The fits are inspected to ensure that the reactions are linear to a correlation coefficient of 0.9. IC₅₀ values are calculated by fitting percent remaining activity vs log (inhibitor concentration) using four-parameter dose–response model (SigmaPlot Version 11.0).

CCR5 Receptor Antagonism Assay. The transfection for the generation of the HEK 293 Glosensor cells stably expressing CCR-5 was carried out using CCR-5 plasmid obtained from the cDNA.org library (CCR050TN00) and Lipofectamine according to the manufacturers' instructions. Transfected cells were subjected to selective pressure for 2–3 weeks through the addition of 1 mg·mL⁻¹ G418. HEK 293 Glosensor cells expressing CCR-5 with a density of 2.5 × 10⁴ cells/mL were placed in each well of a 96 well black plate (100 μL) were incubated at 37 °C, 5% CO₂ for 48 h prior to the assay. On the day of experiment the medium was aspirated and replaced with assay buffer prepared by adding glucose (90 mg) and BSA (50 mg) to 50 mL 1 × HBSS and probenecid solution (180 mg probenecid, 1.25 mL 1 M NaOH and 1.25 mL assay buffer, 500 μL) (complete assay buffer). The complete assay buffer (10 mL) was supplemented by 23 μL Fluo-4 dye (prepared by adding 23 μL DMSO and 23 μL pluronic acid 20% in DMSO to Fluo-4 AM) (Fluo-4 buffer). Fluo-4 buffer (100 μL) was added to each well of the black walled plate and incubated at 37 °C for 45 min. Antagonist (compound) solutions were prepared by either a single concentration (300 nM (48) or 10 μM (49) in complete assay buffer) The Fluo-4 buffer was aspirated and the cells were washed (x2) with complete assay buffer. Complete assay buffer (100 μL) was added to the wells and 10 μL of the corresponding concentration of the antagonist was added in triplicate and incubated for 30 min at 37 °C to give final concentrations of 30 nM or 1 μM. Agonist concentrations for the dose response curve were prepared as serial dilutions with final concentrations of 100 nM – 1 nM in half logs (RANTES). Agonist concentrations (20 μL) were added in triplicate into a clear 96 well plate and were added directly prior to the measurement. The wells were screened on the Flexstation 1 (Molecular Devices) by measuring intracellular calcium by monitoring the change in fluorescence every 2s for 5 min. The estimated affinity value for each antagonist (pK_D) was calculated from the shift of the agonist dose response curve brought about by addition of a single concentration of antagonist (30 nM or 1 μM) using the Gaddum equation as previously described.⁴⁰

PI3K Inhibition Assay. Inhibition of PI3K α, β, γ, and δ enzymatic activity was determined using a homogeneous time-resolved fluorescence (HTRF) kit assay format provided by Millipore.⁵⁴

Molecular Docking—General Methods. The three-dimensional coordinates of the cocrystal structure of sitagliptin in the active site of DPP4 (pdb code 1 × 70), the cocrystal structure of maraviroc in the active site of the chemokine receptor CCR-5 (pdb code 4MB5) and the crystal structure of PI3K δ in complex with pictilisib (pdb code 2WXP) were retrieved from the Protein Data Bank.⁶⁴ All nonprotein atoms, including water and sugar molecules were removed from the model. Using MAKE RECEPTOR 3.0.0 software (OpenEye Scientific Software) an active site model was prepared for each active site (DPP-4, CCR5, PI3K δ) being considered. No constraints were used during this preparation of the receptor model. A database composed of suggested compounds for docking and the reference ligands [sitagliptin (DPP-4), maraviroc (CCR5), pictilisib (PI3K δ)] and the newly designed compounds were processed with the Omega 2.5.1.4 software (OpenEye Scientific Software, Inc.) to generate the 200 lowest energy conformations for each compound. Finally, the compounds were docked into the active site models using the FRED 3.0.1 software and the Chemgauss4 scoring function (OpenEye Scientific Software, Inc.). The docking was visually analyzed for the top 5 best scored poses for the conformation of the designed compounds using VIDA 4.3.0 and outputs visualized using PyMOL (The PyMOL Molecular Graphics System, Version 1.8 Schrödinger, LLC). The poses were visually compared with the cocrystallized reference ligand and the best overlaying docking pose has been presented in this manuscript.

■ ASSOCIATED CONTENT

Supporting Information

The Supporting Information is available free of charge on the ACS Publications website at DOI: 10.1021/acs.jmedchem.6b01801.

Molecular formula strings (CSV)

AUTHOR INFORMATION

Corresponding Author

*E-mail: michael.stocks@nottingham.ac.uk. Tel +44 (0)115 951 5151.

ORCID

Michael J. Stocks: 0000-0003-3046-137X

Notes

The authors declare no competing financial interest.

ACKNOWLEDGMENTS

We acknowledge Jackie Glenn (UoN) for assistance in setting up the CCR5 assay, Jonathan Fray (UoN) for helpful discussions over the PI3K project, Jinqiao Wan, Hongmei Song, and Xiao Hu (HitGen) for their help in assaying of the compounds (DPP4), Simon Hirst and Stephanie Barlow (Sygnature Discovery) for their assistance in the separation of the diastereoisomers using chiral HPLC, and Dan Baillache (GSK) for registering and formatting compounds.

ABBREVIATIONS USED

°C, degrees Celsius; ADME, absorption, distribution, metabolism, and excretion; BOC, boc, *tert*-butoxycarbonyl; CCR5, C–C chemokine receptor type 5; cLogP, calculated logP; compd, compound; DCM, dichloromethane; DMF, dimethylformamide; DPP-4, dipeptidyl peptidase-4; ESI, electrospray ionization; EtOAc, ethyl acetate; GPCR, G protein-coupled receptor; HCl, hydrochloric acid; HIV, human immunodeficiency virus; HPLC, high-performance liquid chromatography; high-pressure liquid chromatography; LIPE, lipophilic ligand efficiency; LCMS, liquid chromatography mass spectrometry; MeCN, acetonitrile; MeOH, methanol; MS, mass spectrometry; NMR, nuclear magnetic resonance; PI3K, phosphoinositide 3-kinase; PIP3, phosphatidylinositol (3,4,5)-triphosphate; RANTES, regulated on activation, normal T cell expressed and secreted; TPSA, topological polar surface area

REFERENCES

- (1) Stocks, M. J.; Wilden, G. R. H.; Pairaudeau, G.; Perry, M. W. D.; Steele, J.; Stonehouse, J. P. A Practical Method for Targeted Library Design Balancing Lead-like Properties with Diversity. *ChemMedChem* **2009**, *4* (5), 800–808.
- (2) Stocks, M.; Hamza, D.; Pairaudeau, G.; Stonehouse, J.; Thorne, P. Concise Synthesis of Novel 2,6-Diazaspiro[3.3]heptan-1-Ones and Their Conversion into 2,6-Diazaspiro[3.3]heptanes. *Synlett* **2007**, *2007* (16), 2587–2589.
- (3) Hamza, D.; Stocks, M.; Décor, A.; Pairaudeau, G.; Stonehouse, J. Synthesis of Novel 2,6-Diazaspiro[3.3]heptanes. *Synlett* **2007**, *2007* (16), 2584–2586.
- (4) Stocks, M. J.; Cheshire, D. R.; Reynolds, R. Efficient and Regiospecific One-Pot Synthesis of Substituted 1,2,4-Triazoles. *Org. Lett.* **2004**, *6* (17), 2969–2971.
- (5) Welsch, M. E.; Snyder, S. a; Stockwell, B. R. Privileged Scaffolds for Library Design and Drug Discovery. *Curr. Opin. Chem. Biol.* **2010**, *14* (3), 347–361.
- (6) Marson, C. M. New and Unusual Scaffolds in Medicinal Chemistry. *Chem. Soc. Rev.* **2011**, *40* (11), 5514–5533.
- (7) DeSimone, R.; Currie, K.; Mitchell, S.; Darrow, J.; Pippin, D. Privileged Structures: Applications in Drug Discovery. *Comb. Chem. High Throughput Screening* **2004**, *7* (5), 473–493.
- (8) Evans, B. E.; Rittle, K. E.; Bock, M. G.; DiPardo, R. M.; Freidinger, R. M.; Whitter, W. L.; Lundell, G. F.; Veber, D. F.; Anderson, P. S. Methods for Drug Discovery: Development of Potent,

Selective, Orally Effective Cholecystokinin Antagonists. *J. Med. Chem.* **1988**, *31* (12), 2235–2246.

(9) Burgey, C.; Deng, J. Z.; Nguyen, D. N.; Paone, D. V.; Potteiger, C. M.; Vacca, J. P. Biarylcarboxamides as P2 × 3 Receptor Antagonists for Treatment of Pain and Their Preparation. WO 2009058298, 2009.

(10) Hoveyda, H. R.; Fraser, G. L.; Roy, M.-O.; Dutheuil, G.; Batt, F.; El Bousmaqui, M.; Korac, J.; Lenoir, F.; Lapin, A.; Noël, S.; Blanc, S. Discovery and Optimization of Novel Antagonists to the Human Neurokinin-3 Receptor for the Treatment of Sex-Hormone Disorders (Part I). *J. Med. Chem.* **2015**, *58* (7), 3060–3082.

(11) Ryckmans, T.; Edwards, M. P.; Horne, V. A.; Correia, A. M.; Owen, D. R.; Thompson, L. R.; Tran, I.; Tutt, M. F.; Young, T. Rapid Assessment of a Novel Series of Selective CB2 Agonists Using Parallel Synthesis Protocols: A Lipophilic Efficiency (LipE) Analysis. *Bioorg. Med. Chem. Lett.* **2009**, *19* (15), 4406–4409.

(12) Tallant, M. D.; Duan, M.; Freeman, G. A.; Ferris, R. G.; Edelstein, M. P.; Kazmierski, W. M.; Wheelan, P. J. Synthesis and Evaluation of 2-Phenyl-1,4-Butanediamine-Based CCR5 Antagonists for the Treatment of HIV-1. *Bioorg. Med. Chem. Lett.* **2011**, *21* (5), 1394–1398.

(13) Hu, Y.; Bajorath, J. How Promiscuous Are Pharmaceutically Relevant Compounds? A Data-Driven Assessment. *AAPS J.* **2013**, *15* (1), 104–111.

(14) Leeson, P. D.; Springthorpe, B. The Influence of Drug-like Concepts on Decision-Making in Medicinal Chemistry. *Nat. Rev. Drug Discovery* **2007**, *6* (11), 881–890.

(15) Oprea, T. I.; Allu, T. K.; Fara, D. C.; Rad, R. F.; Ostopovici, L.; Bologna, C. G. Lead-Like, Drug-like or “Pub-Like”: How Different Are They? *J. Comput.-Aided Mol. Des.* **2007**, *21* (1–3), 113–119.

(16) Muegge, I. Selection Criteria for Drug-like Compounds. *Med. Res. Rev.* **2003**, *23* (3), 302–321.

(17) Schwehm, C.; Li, J.; Song, H.; Hu, X.; Kellam, B.; Stocks, M. J. Synthesis of New DPP-4 Inhibitors Based on a Novel Tricyclic Scaffold. *ACS Med. Chem. Lett.* **2015**, *6* (3), 324–328.

(18) Flatt, P. R.; Bailey, C. J.; Green, B. D. Dipeptidyl Peptidase IV (DPP IV) and Related Molecules in Type 2 Diabetes. *Front. Biosci., Landmark Ed.* **2008**, *13* (January 2016), 3648–3660.

(19) Kim, D.; Wang, L.; Beconi, M.; Eiermann, G. J.; Fisher, M. H.; He, H.; Hickey, G. J.; Kowalchick, J. E.; Leiting, B.; Lyons, K.; Marsilio, F.; McCann, M. E.; Patel, R. A.; Petrov, A.; Scapin, G.; Patel, S. B.; Roy, R. S.; Wu, J. K.; Wyvratt, M. J.; Zhang, B. B.; Zhu, L.; Thornberry, N. A.; Weber, A. E. (2 R)-4-Oxo-4-[3-(Trifluoromethyl)-5,6-dihydro[1,2,4]triazolo[4,3- a]pyrazin- 7(8 H)-Yl]-1-(2,4,5-Trifluorophenyl)butan-2-Amine: A Potent, Orally Active Dipeptidyl Peptidase IV Inhibitor for the Treatment of Type 2 Diabetes. *J. Med. Chem.* **2005**, *48* (1), 141–151.

(20) Biftu, T.; Sinha-Roy, R.; Chen, P.; Qian, X.; Feng, D.; Kuethe, J. T.; Scapin, G.; Gao, Y. D.; Yan, Y.; Krueger, D.; Bak, A.; Eiermann, G.; He, J.; Cox, J.; Hicks, J.; Lyons, K.; He, H.; Salituro, G.; Tong, S.; Patel, S.; Doss, G.; Petrov, A.; Wu, J.; Xu, S. S.; Sewall, C.; Zhang, X.; Zhang, B.; Thornberry, N. a; Weber, A. E. Omarigliptin (MK-3102): A Novel Long-Acting DPP-4 Inhibitor for Once-Weekly Treatment of Type 2 Diabetes. *J. Med. Chem.* **2014**, *57* (8), 3205–3212.

(21) Shu, C.; Ge, H.; Song, M.; Chen, J.-H.; Zhou, H.; Qi, Q.; Wang, F.; Ma, X.; Yang, X.; Zhang, G.; Ding, Y.; Zhou, D.; Peng, P.; Shih, C.-K.; Xu, J.; Wu, F. Discovery of Imigliptin, a Novel Selective DPP-4 Inhibitor for the Treatment of Type 2 Diabetes. *ACS Med. Chem. Lett.* **2014**, *5* (8), 921–926.

(22) Jiang, T.; Zhou, Y.; Chen, Z.; Sun, P.; Zhu, J.; Zhang, Q.; Wang, Z.; Shao, Q.; Jiang, X.; Li, B.; Chen, K.; Jiang, H.; Wang, H.; Zhu, W.; Shen, J. Design, Synthesis, and Pharmacological Evaluation of Fused β -Homophenylalanine Derivatives as Potent DPP-4 Inhibitors. *ACS Med. Chem. Lett.* **2015**, *6* (5), 602–606.

(23) Shan, Z.; Peng, M.; Fan, H.; Lu, Q.; Lu, P.; Zhao, C.; Chen, Y. Discovery of Potent Dipeptidyl Peptidase IV Inhibitors Derived from β -Aminoamides Bearing Substituted [1,2,3]-Triazolopiperidines for the Treatment of Type 2 Diabetes. *Bioorg. Med. Chem. Lett.* **2011**, *21* (6), 1731–1735.

- (24) Catalano, J. G.; Gudmundsson, K. S.; Svolto, A.; Boggs, S. D.; Miller, J. F.; Spaltenstein, A.; Thomson, M.; Wheelan, P.; Minick, D. J.; Phelps, D. P.; Jenkinson, S. Synthesis of a Novel Tricyclic 1,2,3,4,4a,5,6,10b-Octahydro-1,10-Phenanthroline Ring System and CXCR4 Antagonists with Potent Activity against HIV-1. *Bioorg. Med. Chem. Lett.* **2010**, *20* (7), 2186–2190.
- (25) Baxter, E. W.; Reitz, A. B. Reductive Aminations of Carbonyl Compounds with Borohydride and Borane Reducing Agents. In *Organic Reactions*; John Wiley & Sons, Inc.: Hoboken, NJ, USA, 2002; pp 1–714.
- (26) Molecular Conformations Were Generated Using OMEGA and Docking Studies Undertaken with FRED OpenEye's Docking and Scoring Application Version 2.4.6; OpenEye Scientific Software: Santa Fe, NM, <https://www.eyesopen.com>. April 21, 2014.
- (27) Schwehm, C.; Lewis, W.; Blake, A. J.; Kellam, B.; Stocks, M. J. Preparation and Structural Analysis of (±)- Cis -Ethyl 2-Sulfanylidenedecahydro-1,6-Naphthyridine-6-Carboxylate and (±)-Trans -Ethyl 2-Oxooctahydro-1 H -pyrrolo[3,2- c]Pyridine-5-Carboxylate. *Acta Crystallogr., Sect. C: Struct. Chem.* **2014**, *70* (12), 1161–1168.
- (28) Lipinski, C. A. Drug-like Properties and the Causes of Poor Solubility and Poor Permeability. *J. Pharmacol. Toxicol. Methods* **2000**, *44* (1), 235–249.
- (29) Shiao, H.-Y.; Coumar, M. S.; Chang, C.-W.; Ke, Y.-Y.; Chi, Y.-H.; Chu, C.-Y.; Sun, H.-Y.; Chen, C.-H.; Lin, W.-H.; Fung, K.-S.; Kuo, P.-C.; Huang, C.-T.; Chang, K.-Y.; Lu, C.-T.; Hsu, J. T. a; Chen, C.-T.; Jiaang, W.-T.; Chao, Y.-S.; Hsieh, H.-P. Optimization of Ligand and Lipophilic Efficiency To Identify an in Vivo Active Furano-Pyrimidine Aurora Kinase Inhibitor. *J. Med. Chem.* **2013**, *56* (13), 5247–5260.
- (30) Edwards, M. P.; Price, D. A. Role of Physicochemical Properties and Ligand Lipophilicity Efficiency in Addressing Drug Safety Risks. *Annu. Rep. Med. Chem.* **2010**, *45*, 380–391.
- (31) Hopkins, A. L.; Keserü, G. M.; Leeson, P. D.; Rees, D. C.; Reynolds, C. H. The Role of Ligand Efficiency Metrics in Drug Discovery. *Nat. Rev. Drug Discovery* **2014**, *13* (2), 105–121.
- (32) Instant JChem Was Used for Structure Database Management, Search and Prediction. Instant JChem 16.2.15.0 2016, ChemAxon (<https://www.chemaxon.com>). February 11, 2016.
- (33) Hann, M. M. Molecular Obesity, Potency and Other Addictions in Drug Discovery. *MedChemComm* **2011**, *2* (5), 349.
- (34) Thelen, M. Dancing to the Tune of Chemokines. *Nat. Immunol.* **2001**, *2* (2), 129–134.
- (35) Kuritzkes, D.; Kar, S.; Kirkpatrick, P. Maraviroc. *Nat. Rev. Drug Discovery* **2008**, *7* (1), 15–16.
- (36) Dorr, P.; Stammen, B.; van der Ryst, E. Discovery and Development of Maraviroc, a CCR5 Antagonist for the Treatment of HIV Infection. In *Case Studies in Modern Drug Discovery*; Xianhai Huang, R. G. A., Ed.; John Wiley & Sons Inc.: Hoboken, NJ, 2012; pp 216–246.
- (37) Dong, M.; Lu, L.; Li, H.; Wang, X.; Lu, H.; Jiang, S.; Dai, Q. Design, Synthesis, and Biological Activity of Novel 1,4-Disubstituted Piperidine/piperazine Derivatives as CCR5 Antagonist-Based HIV-1 Entry Inhibitors. *Bioorg. Med. Chem. Lett.* **2012**, *22* (9), 3284–3286.
- (38) Tan, Q.; Zhu, Ya; Li, J.; Chen, Z.; Won Han, G.; Kufareva, I.; Li, T.; Ma, L.; Fenalti, G.; Li, J.; Zhang, W.; Xie, X.; Yang, H.; J, H.; Cherezov, V. 3 Hong Liu, Raymond C. Stevens, Qiang Zhao, B. W. Structure of the CCR5 Chemokine Receptor - HIV Entry Inhibitor Maraviroc Complex. *Science* **2013**, *341* (September), 1387–1390.
- (39) Zhao, G.-L.; Lin, S.; Korotvička, A.; Deiana, L.; Kullberg, M.; Córdova, A. Asymmetric Synthesis of Maraviroc (UK-427,857). *Adv. Synth. Catal.* **2010**, *352* (13), 2291–2298.
- (40) Vernall, A. J.; Stoddart, L. A.; Briddon, S. J.; Hill, S. J.; Kellam, B. Highly Potent and Selective Fluorescent Antagonists of the Human Adenosine A 3 Receptor Based on the 1,2,4-Triazolo[4,3- a]Quinoxalin-1-One Scaffold. *J. Med. Chem.* **2012**, *55* (4), 1771–1782.
- (41) Jonathan Fray, M.; Macdonald, S. J. F.; Baldwin, I. R.; Barton, N.; Brown, J.; Campbell, I. B.; Churcher, I.; Coe, D. M.; Cooper, A. W. J.; Craven, A. P.; Fisher, G.; Inglis, G. G. A.; Kelly, H. A.; Liddle, J.; Maxwell, A. C.; Patel, V. K.; Swanson, S.; Wellaway, N. A Practical Drug Discovery Project at the Undergraduate Level. *Drug Discovery Today* **2013**, *18* (23–24), 1158–1172.
- (42) Ito, K.; Caramori, G.; Adcock, I. M. Therapeutic Potential of Phosphatidylinositol 3-Kinase Inhibitors in Inflammatory Respiratory Disease. *J. Pharmacol. Exp. Ther.* **2007**, *321* (1), 1–8.
- (43) Thorpe, L. M.; Yuzugullu, H.; Zhao, J. J. PI3K in Cancer: Divergent Roles of Isoforms, Modes of Activation and Therapeutic Targeting. *Nat. Rev. Cancer* **2014**, *15* (1), 7–24.
- (44) Fransecky, L.; Mochmann, L. H.; Baldus, C. D. Outlook on PI3K/AKT/mTOR Inhibition in Acute Leukemia. *Mol. Cell. Ther.* **2015**, *3* (1), 2.
- (45) Gutierrez, A.; Sanda, T.; Grebliunaite, R.; Carracedo, A.; Salmena, L.; Ahn, Y.; Dahlberg, S.; Neuberg, D.; Moreau, L. A.; Winter, S. S.; Larson, R.; Zhang, J.; Protopopov, A.; Chin, L.; Pandolfi, P. P.; Silverman, L. B.; Hunger, S. P.; Sallan, S. E.; Look, A. T. High Frequency of PTEN, PI3K, and AKT Abnormalities in T-Cell Acute Lymphoblastic Leukemia. *Blood* **2009**, *114* (3), 647–650.
- (46) Lee, K. S.; Park, S. J.; Kim, S. R.; Min, K. H.; Jin, S. M.; Puri, K. D.; Lee, Y. C. Phosphoinositide 3-Kinase-δ Inhibitor Reduces Vascular Permeability in a Murine Model of Asthma. *J. Allergy Clin. Immunol.* **2006**, *118* (2), 403–409.
- (47) Folkes, A. J.; Ahmadi, K.; Alderton, W. K.; Alix, S.; Baker, S. J.; Box, G.; Chuckowree, I. S.; Clarke, P. A.; Depledge, P.; Eccles, S. A.; Friedman, L. S.; Hayes, A.; Hancox, T. C.; Kugendradas, A.; Lensun, L.; Moore, P.; Olivero, A. G.; Pang, J.; Patel, S.; Pergl-Wilson, G. H.; Raynaud, F. I.; Robson, A.; Saghir, N.; Salphati, L.; Sohal, S.; Ultsch, M. H.; Valenti, M.; Wallweber, H. J. A.; Wan, N. C.; Wiesmann, C.; Workman, P.; Zhyvoloup, A.; Zvebil, M. J.; Shuttleworth, S. J. The Identification of 2-(1 H -Indazol-4-Yl)-6-(4-Methanesulfonyl-Piperazin-1-Ylmethyl)-4-Morpholin-4-Yl-thieno[3,2- D]Pyrimidine (GDC-0941) as a Potent, Selective, Orally Bioavailable Inhibitor of Class I PI3 Kinase for the Treatment of Cancer †. *J. Med. Chem.* **2008**, *51* (18), 5522–5532.
- (48) Berndt, A.; Miller, S.; Williams, O.; Le, D. D.; Houseman, B. T.; Pacold, J. I.; Gorrec, F.; Hon, W.; Liu, Y.; Rommel, C.; Gaillard, P.; Rückle, T.; Schwarz, M. K.; Shokat, K. M.; Shaw, J. P.; Williams, R. L. The p110δ Structure: Mechanisms for Selectivity and Potency of New PI(3)K Inhibitors. *Nat. Chem. Biol.* **2010**, *6* (2), 117–124.
- (49) Sutherland, D. P.; Baker, S.; Bisconte, A.; Blaney, P. M.; Brown, A.; Chan, B. K.; Chantry, D.; Castaneda, G.; DePledge, P.; Goldsmith, P.; Goldstein, D. M.; Hancox, T.; Kaur, J.; Knowles, D.; Kondru, R.; Lesnick, J.; Lucas, M. C.; Lewis, C.; Murray, J.; Nadin, A. J.; Nonomiya, J.; Pang, J.; Pegg, N.; Price, S.; Reif, K.; Safina, B. S.; Salphati, L.; Staben, S.; Seward, E. M.; Shuttleworth, S.; Sohal, S.; Sweeney, Z. K.; Ultsch, M.; Waszkowycz, B.; Wei, B. Potent and Selective Inhibitors of PI3Kδ: Obtaining Isoform Selectivity from the Affinity Pocket and Tryptophan Shelf. *Bioorg. Med. Chem. Lett.* **2012**, *22* (13), 4296–4302.
- (50) Heffron, T. P.; Heald, R. A.; Ndubaku, C.; Wei, B.; Augustin, M.; Do, S.; Edgar, K.; Eigenbrot, C.; Friedman, L.; Gancia, E.; Jackson, P. S.; Jones, G.; Kolesnikov, A.; Lee, L. B.; Lesnick, J. D.; Lewis, C.; McLean, N.; Mörtl, M.; Nonomiya, J.; Pang, J.; Price, S.; Prior, W. W.; Salphati, L.; Sideris, S.; Staben, S. T.; Steinbacher, S.; Tsui, V.; Wallin, J.; Sampath, D.; Olivero, A. G. The Rational Design of Selective Benzoxazepin Inhibitors of the α-Isoform of Phosphoinositide 3-Kinase Culminating in the Identification of (S)-2-((2-(1-Isopropyl-1 H -1,2,4-Triazol-5-Yl)-5,6-Dihydrobenzo[F]imidazo[1,2- D][[1,4]-oxazepin-9-Yl)oxy)propa. *J. Med. Chem.* **2016**, *59* (3), 985–1002.
- (51) Sato, S.; Sakamoto, T.; Miyazawa, E.; Kikugawa, Y. One-Pot Reductive Amination of Aldehydes and Ketones with α-Picoline-Borane in Methanol, in Water, and in Neat Conditions. *Tetrahedron* **2004**, *60* (36), 7899–7906.
- (52) Miyaura, N.; Yamada, K.; Suzuki, A. A New Stereospecific Cross-Coupling by the Palladium-Catalyzed Reaction of 1-Alkenylboranes with 1-Alkenyl or 1-Alkynyl Halides. *Tetrahedron Lett.* **1979**, *20* (36), 3437–3440.
- (53) Miyaura, N.; Suzuki, A. Stereoselective Synthesis of Arylated (E)-Alkenes by the Reaction of Alk-1-Enylboranes with Aryl Halides in

the Presence of Palladium Catalyst. *J. Chem. Soc., Chem. Commun.* **1979**, No. No. 19, 866.

(54) Down, K.; Amour, A.; Baldwin, I. R.; Cooper, A. W. J.; Deakin, A. M.; Felton, L. M.; Guntrip, S. B.; Hardy, C.; Harrison, Z. A.; Jones, K. L.; Jones, P.; Keeling, S. E.; Le, J.; Livia, S.; Lucas, F.; Lunniss, C. J.; Parr, N. J.; Robinson, E.; Rowland, P.; Smith, S.; Thomas, D. A.; Vitulli, G.; Washio, Y.; Hamblin, J. N. Optimization of Novel Indazoles as Highly Potent and Selective Inhibitors of Phosphoinositide 3-Kinase δ for the Treatment of Respiratory Disease. *J. Med. Chem.* **2015**, *58* (18), 7381–7399.

(55) Dossetter, A. G.; Griffen, E. J.; Leach, A. G. Matched Molecular Pair Analysis in Drug Discovery. *Drug Discovery Today* **2013**, *18* (15–16), 724–731.

(56) Ritchie, T. J.; Luscombe, C. N.; Macdonald, S. J. F. Analysis of the Calculated Physicochemical Properties of Respiratory Drugs: Can We Design for Inhaled Drugs Yet? *J. Chem. Inf. Model.* **2009**, *49* (4), 1025–1032.

(57) Ball, J.; Archer, S.; Ward, S. PI3K Inhibitors as Potential Therapeutics for Autoimmune Disease. *Drug Discovery Today* **2014**, *19* (8), 1195–1199.

(58) Foster, J. G.; Blunt, M. D.; Carter, E.; Ward, S. G. Inhibition of PI3K Signaling Spurs New Therapeutic Opportunities in Inflammatory/Autoimmune Diseases and Hematological Malignancies. *Pharmacol. Rev.* **2012**, *64* (4), 1027–1054.

(59) Vanhaesebroeck, B.; Whitehead, M. A.; Piñeiro, R. Molecules in Medicine Mini-Review: Isoforms of PI3K in Biology and Disease. *J. Mol. Med.* **2016**, *94* (1), 5–11.

(60) Taylor, R. D.; MacCoss, M.; Lawson, A. D. G. Rings in Drugs. *J. Med. Chem.* **2014**, *57* (14), 5845–5859.

(61) Goldberg, F. W.; Kettle, J. G.; Kogej, T.; Perry, M. W. D.; Tomkinson, N. P. Designing Novel Building Blocks Is an Overlooked Strategy to Improve Compound Quality. *Drug Discovery Today* **2015**, *20* (1), 11–17.

(62) Bembenek, S. D.; Tounge, B. A.; Reynolds, C. H. Ligand Efficiency and Fragment-Based Drug Discovery. *Drug Discovery Today* **2009**, *14* (5–6), 278–283.

(63) Wang, A.; Dorso, C.; Kopcho, L.; Locke, G.; Langish, R.; Harstad, E.; Shipkova, P.; Marcinkeviciene, J.; Hamann, L.; Kirby, M. S. Potency, Selectivity and Prolonged Binding of Saxagliptin to DPP4: Maintenance of DPP4 Inhibition by Saxagliptin in Vitro and Ex Vivo When Compared to a Rapidly-Dissociating DPP4 Inhibitor. *BMC Pharmacol.* **2012**, *12* (1), 2.

(64) RCSB Protein Data Bank, <http://www.rcsb.org/pdb/home/home.do>. April 18, 2014.